Genderjahn, S., Alawi, M., Wagner, D., Schüller, I., Wanke, A., Mangelsdorf, K. (2018): Microbial Community Responses to Modern Environmental and Past Climatic Conditions in Omongwa Pan, Western Kalahari: A Paired 16S rRNA Gene Profiling and Lipid Biomarker Approach. - *Journal of Geophysical Research*, *123*, 4, pp. 1333—1351.

DOI: http://doi.org/10.1002/2017JG004098

Journal of Geophysical Research: Biogeosciences

RESEARCH ARTICLE
10.1002/2017JG004098

Key Points:
- Kalahari pan structures possess high potential to act as geoarchives for preserved biomolecules in arid to semiarid regions
- Past microbial biomarker suggests changing climatic conditions during the Late Glacial to Holocene transition in the western Kalahari
- Based on taxonomic investigations, the abundance and diversity of the microbial community in the pan is related to near-surface processes

Supporting Information:
- Supporting Information S1

Correspondence to:
S. Genderjahn,
steffi.genderjahn@gfz-potsdam.de

Citation:
Genderjahn, S., Alawi, M., Wagner, D., Schüller, I., Wanke, A., & Mangelsdorf, K. (2018). Microbial community responses to modern environmental and past climatic conditions in Omongwa Pan, western Kalahari: A paired 16S rRNA gene profiling and lipid biomarker approach. *Journal of Geophysical Research: Biogeosciences*, *123*, 1333–1351. https://doi.org/10.1002/2017JG004098

Received 4 AUG 2017
Accepted 22 MAR 2018
Accepted article online 26 MAR 2018
Published online 22 APR 2018

Microbial Community Responses to Modern Environmental and Past Climatic Conditions in Omongwa Pan, Western Kalahari: A Paired 16S rRNA Gene Profiling and Lipid Biomarker Approach

S. Genderjahn[1], M. Alawi[1], D. Wagner[1,2], I. Schüller[3], A. Wanke[4], and K. Mangelsdorf[1]

[1]GFZ German Research Centre for Geosciences, Helmholtz Centre Potsdam, Potsdam, Germany, [2]Institute of Earth and Environmental Science, University of Potsdam, Potsdam, Germany, [3]Marine Research Department, Senckenberg am Meer, Wilhelmshaven, Germany, [4]Department of Geology, University of Namibia, Windhoek, Namibia

Abstract Due to a lack of well-preserved terrestrial climate archives, paleoclimate studies are sparse in southwestern Africa. Because there are no perennial lacustrine systems in this region, this study relies on a saline pan as an archive for climate information in the western Kalahari (Namibia). Molecular biological and biogeochemical analyses were combined to examine the response of indigenous microbial communities to modern and past climate-induced environmental conditions. The 16S rRNA gene high-throughput sequencing was applied to sediment samples from Omongwa pan to characterize the modern microbial diversity. Highest diversity of microorganisms, dominated by the extreme halophilic archaeon *Halobacteria* and by the bacterial phylum *Gemmatimonadetes*, was detected in the near-surface sediments of Omongwa pan. In deeper sections abundance and diversity significantly decreases and *Bacillus*, known to form spores, become dominant. Lipid biomarkers for living and past microbial life were analyzed to track the influence of climate variation on the abundance of microbial communities from the Last Glacial Maximum to Holocene time. Since water is an inevitable requirement for microbial life, in this dry region the abundance of past microbial biomarkers was evaluated to conclude on periods of increased paleoprecipitation in the past. The data point to a period of increased humidity in the western Kalahari during the Last Glacial to Holocene transition indicating a southward shift of the Intertropical Convergence Zone during this period. Comparison with results from a southwestern Kalahari pan suggests complex displacements of the regional atmospheric systems since the Last Glacial Maximum.

1. Introduction

The arid southern African landscape is characterized by saline pans. These low-relief, closed basins are characteristic forms in the semiarid to arid regions of eastern Namibia, northwestern Botswana, and northern and western South Africa (Lancaster, 1986). Occasionally strong precipitation leads to transient runoff in ephemeral rivers and rising saline groundwater. In consequence, pans are filled temporally with water from several days up to a few weeks depending on the amount of precipitation. Solutes which are produced and deposited on the continent are stored within an internal drainage system to form saline pans (Goudie & Thomas, 1985). Local environmental factors such as precipitation, rainwater inflow, and eolian activity can substantially influence the sedimentology and morphology of pan structures (Roy et al., 2006). Sedimentary processes such as flooding and evapoconcentration can form different types of strata that serve as paleoclimatic archives (Lowenstein & Hardie, 1985). Thus, in dry environments without perennial aquatic systems (such as lakes) pan systems may represent geoarchives for climate information (Genderjahn et al., 2017; Telfer et al., 2009).

Precipitation in southern Africa is regulated by the seasonal shift of the Intertropical Convergence Zone (ITCZ) and the westerlies in the Southern Hemisphere (Ahrens & Samson, 2010). The ITCZ is located where both northeastern and southeastern trade winds converged into a narrow belt close to the equator. In austral winter (June to September) the ITCZ is located north of the equator, while in austral summer (December to March) the ITCZ is strongly shifted to the south bringing rain to southern Africa from the Indian Ocean (Ahrens & Samson, 2010). Nowadays, precipitation occurs only occasionally by seasonal rain showers during austral summer (summer rainfall zone, see map in Zhao et al., 2016) in the Kalahari region. In contrast, winter

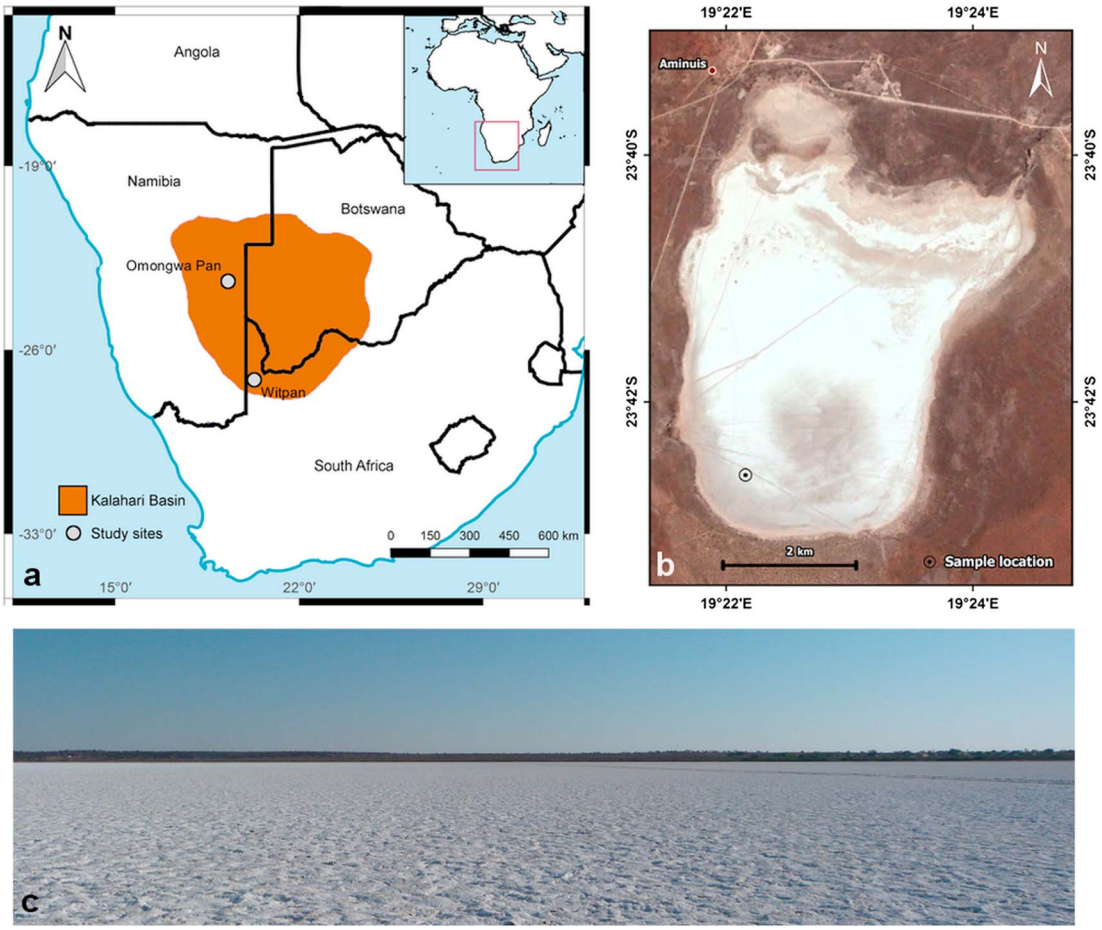

Figure 1. (a) Map of Namibia with the study site Omongwa pan (23°42.46′S, 19°22.15′E) in the western Kalahari. The position of Witpan (26°40.66′S, 20°09.45′E) in the southwestern Kalahari was added for comparison (Genderjahn et al., 2017). (b) Aerial photograph of Omongwa pan with sample location EO-1 Hyperion image (Basemap source: Digital Globe RGB image, September 2013, provided by Google Inc.). (c) Image of Omongwa pan with white saline crust.

rainfall is influenced by the northward expansion of the westerlies transporting moisture only to the western coastline of South Africa (Figure 1a; Chase et al., 2013; Zhao et al., 2016).

Proxy data from paleoenvironmental archives in southwestern Africa are scarce. Most climate data for South West Africa derive from archives such as tufas (Butzer et al., 2017), calcretes (Nash & McLaren, 2003), stromatolites (Lancaster, 1986), fluvial systems (Ramisch et al., 2017), and slack water deposits (Heine, 2004). Nevertheless, these geoarchives are extremely heterogeneous and indicate different regional environmental reactions to climate variations (Heine, 2005). Only a few studies used pan sediments as an appropriate geological record (Genderjahn et al., 2017; Holmgren & Shaw, 1997; Telfer et al., 2009). Genderjahn et al. (2017) showed that Witpan in the southwestern Kalahari represents a geoarchive for biomolecule proxies transporting valuable paleoclimatic information.

Due to at least occasional rainfall and resulting sporadic availability of water pans form a habitat for microbial life. Climate variations and the associated variability of precipitation have a strong influence on the microbial ecosystem in saline pans. Varying temperatures, infrequent precipitation, and therefore low water availability as well as high salinity conditions affect the abundance and adaptation of microbial communities (Makhalanyane et al., 2015; Oren, 2014; Ventosa et al., 2011). Previous studies investigated the microbial communities in extreme saline habitats and demonstrated that microbial diversity significantly varied between different saline pan systems (Jiang et al., 2006; Maturrano et al., 2006; Montoya et al., 2013). It has been also reported that DNA can be preserved within fluid inclusions in halite and gypsum that were formed when sodium chloride starts to precipitate (Benison & Karmanocky, 2014; Sankaranarayanan et al.,

2014). Insights into microbial life in extreme environments improve a more global view of evolutionary adjustment (Johnson et al., 2015). Thus, in dry and saline environments microbial biomarkers are a promising tool to reflect paleoenvironmental and paleoclimatic information, as described by Genderjahn et al. (2017) in the southwestern Kalahari.

Lipid biomarkers are characteristic enough to describe microorganism on a broad taxonomic level, but unsuitable to identify single species (Coolen & Gibson, 2009). Microbial membrane phospholipids (PLs) and their fatty acid (PLFA) side chains represent microbial biomarkers that are indicative for living bacteria (Zelles, 1999). Phospholipids are rapidly degraded after cell death. Therefore, their occurrence indicates the presence of living cells in geological samples (Logemann et al., 2011; White et al., 1979). In contrast to PLFA biomarkers, archaeol and glycerol dialkyl glycerol tetraethers (GDGTs) represent dead or fossil microbial biomass (Pitcher et al., 2009). GDGTs occur ubiquitously in water, soil, and sediments and represent core lipids from past archaea and bacteria (Schouten et al., 2013) in older sediments. During early diagenetic degradation processes intact lipids lose their head groups and the remaining core lipids are very stable and well preserved in sediments over geological time scales (Pease et al., 1998). Branched GDGTs (brGDGTs) are omnipresent compounds in both lake sediments (Blaga et al., 2009) and in soils (Weijers et al., 2007). They are known to be derived from bacteria (Weijers et al., 2006), while isoprenoid GDGTs (isoGDGTs) and dialkyl glycerol diethers such as archaeol are synthesized by archaea (Kates, 1996).

In contrast to bacterial PL esters, intact archaeal cell membrane lipids such as PL archaeols are quite stable due to the fact that their side chains are ether bound. This higher bond stability restricts their use as life marker molecules for archaea (Logemann et al., 2011). Since microbial communities usually consist of both bacteria and archaea, in the current paper the bacterial PLFAs are used as a general marker to trace living microbial communities in the investigated pan deposits.

As lipid biomarkers are limited in their taxonomic resolution, the microbial community in Omongwa pan is described in detail by an Illumina-based 16S rRNA sequencing approach and, additionally, quantitative polymerase chain reaction (PCR) to reveal the abundance of bacteria and archaea. Using next generation sequencing (NGS) microbial taxa can be identified, including uncultivable organisms and those present in low abundance within the microbial community, which may be relevant for functional diversity and ecosystem stability (Kysela et al., 2005; Sogin et al., 2006).

Literature data indicate that in southern Africa the seasonality and amount of precipitation changed to higher precipitation during the Late Glacial Maximum (LGM 21 ± 2 ka) (Gasse et al., 2008). During this time the westerlies moved northward, toward the South African mainland, caused by the expansion of the Antarctic sea ice shield. As a result, the winter rainfall zone has broadened, which affected the precipitation in southwestern Africa during the LGM (Zhao et al., 2016). Previous analyses of microbial lipid biomarker data indicated a period of higher precipitation during the LGM also for the southwestern Kalahari (Genderjahn et al., 2017). However, it is not known how far the northward expansion of the winter rainfall zone affected the paleoprecipitation pattern in the Kalahari region during the LGM.

In this paper we investigate the microbial composition in Omongwa pan deposits as a geoarchive for climatic variations in the western Kalahari region. For the first time, this study characterizes depth-related compositional variations of the indigenous microbial community in a Kalahari pan system with high taxonomic resolution using a DNA approach. Furthermore, based on ^{14}C age data biomarker variations are used to reconstruct paleoprecipitation patterns and evaluate how far the winter rainfall zone was shifted to the north during the LGM. Thus, the combination of applied molecular biological and biogeochemical methods improves our knowledge of the environmental conditions and climatic evolution in eastern Namibia during the LGM to Holocene time period.

2. Material and Methods

2.1. Study Site

Pans (or playas) are a predominant geomorphic feature of the Kalahari, where evaporation exceeds precipitation (Goudie & Wells, 1995; Lancaster, 1976). Omongwa pan (Figure 1b, 23°42.59′S, 19°22.15′E) in the western Kalahari is the largest pan of the Aminius region in eastern Namibia and covers an area of about 20 km^2. This pan is located in a broad belt of pans which spread from the northwest of Botswana to the east of

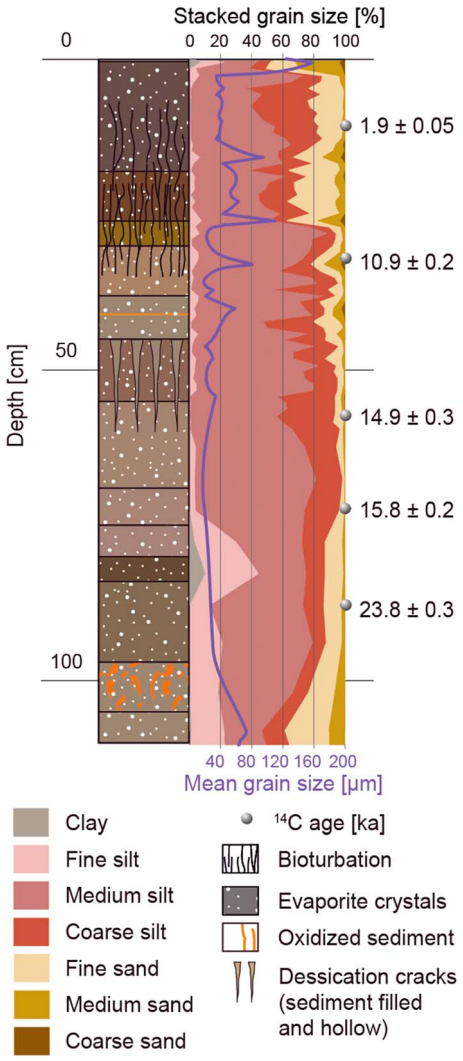

Figure 2. Sedimentological profile with stacked grain size distribution and mean grain size (0–250 µm; violet line) from Omongwa pan. Sediment colors refer to the Munsell soil color chart.

Namibia. This concentration of pans may be linked to a former drainage line of the Nossob River (Lancaster, 1986). Average rainfall at Aminuis is about 200–250 mm per year whereby 90% of the total precipitation occurs during austral summer season between December and April (Mees, 1999; Milewski et al., 2017). Omongwa pan is characterized by low organic matter and low-porosity fine-grained sediments, mostly consisting of medium to coarse silt and gypsum crystals with low variability with depth (Figure 2). Mudcracks occur between 45 and 65 cm depth. In evaporate settings, such as ephemeral saline pans, sedimentary strata is formed due to alternating periods of flooding, evaporative concentration and desiccation (Lowenstein & Hardie, 1985). However, in Omongwa pan no distinct evaporitic layers could be identified and evaporite crystals are dispersed in the deposits. According to Milewski et al. (2017) the main mineralogy components of the top layer at our study site are halite (NaCl, 94%) and gypsum ($CaSO_4{\cdot}2H_2O$, 3%). In semiarid to arid regions, for one thing, water will evaporate quickly before it can infiltrate. On the other hand salt-saturated water seeps into the ground and salts, carbonates, and gypsum crystals concentrate in or on the pan floor (Mees, 1999). In dry months the capillary evaporation of shallow groundwater will accumulate salts near the surface (Smith & Compton, 2004). The surface samples were slightly alkaline with a pH value of ~8 (Milewski et al., 2017).

Nowadays, there are groundwater discharges at the northern and western sides of Omongwa pan, resulting into open waterholes. The top layer is covered by a flat halite crust (Figure 1c) with extremely low coverage (or predominantly absence) of vegetation. There is no substantial inflow, and surface runoff is minimized by the high infiltration rates of the Kalahari sands and the surrounding topography (Milewski et al., 2017). Omongwa pan might not allow permanent standing water, but during rainy periods it is flooded for a short period of several days (Milewski et al., 2017). Modern groundwater table depth was measured around 165 cm.

The high capillary porosity of the surface sand retained the infiltrating rainfall and today no recharge to groundwater takes place (Lancaster, 1976). On the southern margin there is a well-developed lunette dune and at the southwestern side a series of massive calcretes, up to 4 m high, occurs. The calcretes indicate evidence of algal mats and stromatolites at higher levels, which suggest that the calcretes represent previous pan surface levels of groundwater discharge (Lancaster, 1986).

2.2. Sampling and Sample Material

A field campaign was conducted to Namibia in autumn 2013. Omongwa pan samples (23°42.59′S, 19°22.15′E, eastern Namibia, Aminuis region, Figure 1b) were taken from a 50 cm deep trench dug into the pan floor and from a short core (50–205 cm) drilled by an Eijkelkamp hand auger. Within the upper 15 cm sediment samples were taken in 3-cm intervals, followed by 5-cm intervals down to 50 cm, and continued in 10-cm steps down to 105 cm. Sediment samples for microbiological studies from the short core were only taken from the core interior to avoid contamination brought down by the drill equipment. During the field campaign sediment samples for biomarker studies were immediately frozen in liquid nitrogen, transported under these conditions to our home laboratories and finally stored at −24°C until analysis. In total, 18 different depth intervals of Omongwa pan were analyzed for biomarkers. For geochemical characterization and molecular analyses such as DNA analysis samples were stored frozen and were analyzed in replicates. The age data of Omongwa pan was provided by Schüller and Wehrmann (2016) within the GeoArchives project. In total six ^{14}C-radiocarbon dates on bulk total organic carbon (TOC) of Omongwa sediments were obtained (Figure 2). The first two data points revealed Holocene ages with 1.9 ± 0.06 and 10.9 ± 0.22 ka at 10.5- and

32.5-cm depth, respectively. Another age was determined at 57.5-cm depth, yielding 14.9 ± 0.29 ka, which was only slightly younger than the sample from 72.5-cm depth with 15.8 ± 0.25 ka, pointing to increased sedimentation at this interval. At 87.5-cm depth an age of 23.8 ± 0.29 ka was determined, falling into the Last Glacial Maximum (LGM: 21 ± 2 ka). The last age was provided for 205.5-cm depth with 42.4 ± 0.84 ka (Marine Isotope Stage 3). Thus, sediment between 105 and approximately 45 cm fall into the range of the Glacial period (Marine Isotope Stage 2), whereas sediments from 105 to approximately 80 cm represent LGM deposits and from 80 to 45 cm the transition from the LGM to the Holocene (Last Glacial-Holocene transition, 18–11.7 ka). Sediments from ~45 cm to the surface are of Holocene age. The ^{14}C-radiocarbon dates of Omongwa deposits were determined at the Poznań Radiocarbon Laboratory, Poland.

2.3. Sediment Properties

Since sediment samples contained too little pore water, samples were leached according to Blume et al. (2011). Five grams of each sediment sample was suspended in 25 ml of deionized water, shaken for 90 min and centrifuged to remove all solids. Concentrations of anions were measured in at least duplicates by ion chromatography. The leached samples were investigated for chloride (Cl^-), nitrate (NO_3^-), sulfate (SO_4^{2-}), and small organic acid concentrations. Details on the method to detect anions have been described elsewhere (e.g., Noah et al., 2014; Vieth et al., 2008). Analytical settings are shown in supporting information Table S1. For quantification standards runs, which contain all investigated ions, were measured in different concentration once a day. Furthermore, the TOC content of each sediment sample was measured by Potsdamer Wasser und Umweltlabor GmbH & Co. KG, Germany. The water content of each sample was determined by weighing a certain sample amount prior to and after drying.

2.4. DNA Extraction and Preparation of NGS

The total genomic DNA was extracted in triplicate from 0.3 to 0.5 g of ground and homogenized pan sediment samples using the Power Soil™ DNA Isolation Kit (Mo Bio Laboratories Inc., Carlsbad, California, United States), according to the company's protocol. To enhance the efficiency of DNA extraction, all samples were heated up after step four for 10 min at 70°C.

The hypervariable region V4 of the 16S rDNA was targeted for a subsequent amplification using the primer pair 515F and 806R (Caporaso et al., 2011). PCRs were performed in at least analytical triplicates. The PCR reaction mix contained 50 μl Mango-Mix including a MangoTaq™ DNA Polymerase, $MgCl_2$, and ultrapure Deoxyribonucleotide triphosphates (dNTPs) manufactured by Bioline GmbH, Luckenwalde, Germany, 1 μl of each primer (10 mM), and 5 μl template and was filled up to 50 μl with PCR-clean water (MO BIO Laboratories, Inc., Carlsbad, California, United States). To prepare the sediment samples for sequencing, the PCR products were run on a 1% agarose gel in 1X Tris-acetate-EDTA buffer stained with GelRed™ Nucleic Acid Gel Stain (Biotium, United States). PCR products were pooled and purified by Genomic DNA Clean & Concentrator™-10 (Zymo Research, United States) and quantified using the Qubit Fluorometer (Invitrogen™, Thermo Fisher Scientific, United States). Samples from each depth were tagged with two different primer pairs (resulting in duplicates) and were delivered to the Illumina MiSeq platform at Eurofins Genomics, 85560 Ebersberg, Germany. Primer specifications are comprising a 6 bp tag and the primer sequence spanning a region of the V4 domain (*E. coli* reference sequence).

2.5. Processing NGS Data

Assembling of reads was performed by using PEAR (Zhang et al., 2014). Standardizing the nucleotide sequence orientation, trimming, and filtering of low-quality sequences was done by using Trimmomatic (Bolger et al., 2014). Chimeras were removed and sequences were clustered into OTUs (operational taxonomic units). The OTU grouping of sequences was based on a similarity-based clustering with a 97% sequence similarity threshold. The following filters were applied: removing singletons and eliminating all OTUs which had an occurrence of less than 0.5% in each sample. A taxonomic classification was assigned by the SILVA 119 database (www.arb-silva.de) with a cutoff of 97% using the QIIME pipeline via picking open-reference OTUs method (Caporaso et al., 2010). Statistics were carried out by using CANACO 5. With the help of principal component analyses (PCA) and canonical correspondence analysis (CCA) results were explained. PCA is a multivariate technique based on the Euclidean distance among the samples. PCA combines the physical and chemical factors into master variables that explain the most variation in the data set. CCA is a method to describe species-environment relationships and determine environmental factors

which explain alteration in the microbial community composition (Ramette, 2007). Statistics based on relative abundance of OTUs and on standardized environmental parameters. The Shannon index was calculated based on the filtered OTU table using the statistic program PAST 3.15.

2.6. qPCR Analysis of Archaeal and Bacterial SSU rRNA Genes

The small subunit (SSU) rRNA gene copy numbers of bacteria and archaea were calculated by a quantitative PCR (qPCR) approach. The forward primer Eub 331-F 5′-TCCTACGGGAGGCAGCAGT-3′ and reverse primer Eub 797-R 5′-GGACTA CCAGGG-TATCTAATCCTGTT-3′ (Nadkarni et al., 2002) were utilized to amplify fragments from bacterial SSU rRNA genes and for archaea the primer pair A751F 5′-CCg ACG GTG AGR GRY GAA-3′ and UA1204R 5′-TTMGGGGCATRCIKACCT-3′ (Baker et al., 2003) was used. All qPCR reactions were performed in analytical triplicates in a thermo cycler (CFX Connect™ Real-Time PCR Detection System, Bio-Rad Laboratories, United States) instrument using the polymerase iTaq™ Universal SYBR® Green Super Mix (Quiagen). The PCR mix contained 12.5 ml of SYBR® Green Super Mix, 0.5 μl of each primer (20 mM), and 5 μl template (diluted, 1:7) and was filled up to 25 ml with PCR-clean water (MO BIO Laboratories, Inc., Carlsbad, California, United States). The following cycling program was performed: denaturation at 95°C for 30 s, annealing at 58.5°C respectively for 1 min, and elongation at 72°C for 30 s followed by 80°C for 3 s, 40 cycles in total. To generate a standard curve, known dilutions (10^1–10^7 gene copies) of the target fragments amplified from *Bacillus subtilis* (for bacteria) and *Methanosarcina barkeri* (for archaea) were used. Finally, melting curve analyses were done to guarantee correct amplification.

2.7. Lipid Biomarker Analysis

Samples were freeze-dried, ground, and homogenized using a disk-mill with a stainless steel grinding set. Afterward, sediments were extracted by a procedure modified after Bligh and Dyer (1959). The obtained extract was separated into four fractions of different polarity using a sample preparation method according to Zink and Mangelsdorf (2004). The low polar fraction including GDGTS was eluted with 20 ml of chloroform. The free fatty acid was rinsed with 50 ml of methyl formiate blended with 12.5 μl of glacial acetic acid and the glycolipid fraction with 20 ml of acetone. After removal of the Florisil® column the membrane PL fraction was eluted with 25 ml of methanol. To quantify the polar lipids (e.g., PLs), an internal standard, 1-myristoy-(D27)-2-hydroxy-sn-glycerol-3-phosphocholine, was added. The low polar fraction was analyzed by high-performance liquid chromatography-atmospheric pressure chemical ionization-mass spectrometry (HPLC-APCI-MS) for GDGT and archaeol analysis. The PL fraction was saponified to obtain the PLFA, which were measured by gas chromatography-mass spectrometry (GC-MS).

2.8. Detection of Life Markers

Half of the PL fraction was used to gain the PLFAs following a FA cleavage method described in Müller et al. (1990). For GC-MS analyses, the samples were measured on Trace GC Ultra (Thermo Electron Corporation) coupled to a DSQ Thermo Finnigan Quadrupole MS (Thermo Electron Corporation). The GC was equipped with a cold injection system (Thermo Electron Corporation) and a 50 m × 0.22 mm × 0.25 μm Scientific Glass Engineering (SGE) Analytical Science SGE™ BPX5 column and was run in splitless mode using the following program: injector temperature 50–300°C at 10°C s^{-1}, oven program 50–310°C with a rate 3°C min^{-1}, and 310°C held for 30 min. Helium was utilized as carrier gas at a constant flow rate of 1 ml min^{-1}. The GC-MS was run in electron ionization mode at 70 eV. Full-scan mass spectra were recorded from m/z 50–600 amu at a scan rate at 1.5 scans per second.

2.9. Detection of Past Microbial Markers

GDGTs and archaeol were examined by HPLC-APCI-MS using a Shimadzu LC10AD HPLC coupled to a Finningan MAT TSQ 7000 mass spectrometer. The low polar lipid fraction was dissolved in *n*-hexane to precipitate asphaltenes that were removed by filtration over sodium sulfate. Subsequently, the cleaned fraction was separated into an aliphatic, aromatic, and heterocompound fractions using a medium-pressure liquid chromatography system (Radke et al., 2002). The heterocompound fraction containing the GDGTs and archaeol were measured by an HPLC-APCI-MS with the following settings modified after Hopmans et al. (2000). For compound separation a Prevail Cyano column (2.1 × 150 mm, 3 μm; Alltech) equipped with a precolumn filter was used. Compounds of interest were eluted isocratically with a mobile phase consisting of *n*-hexane (99%) and isopropanpol (1%) for 5 min, followed by a linear gradient to 1.8% isopropanol in 40 min and subsequently in 1 min to 10% isopropanol, kept for 5 min to clean the column, set back to initial

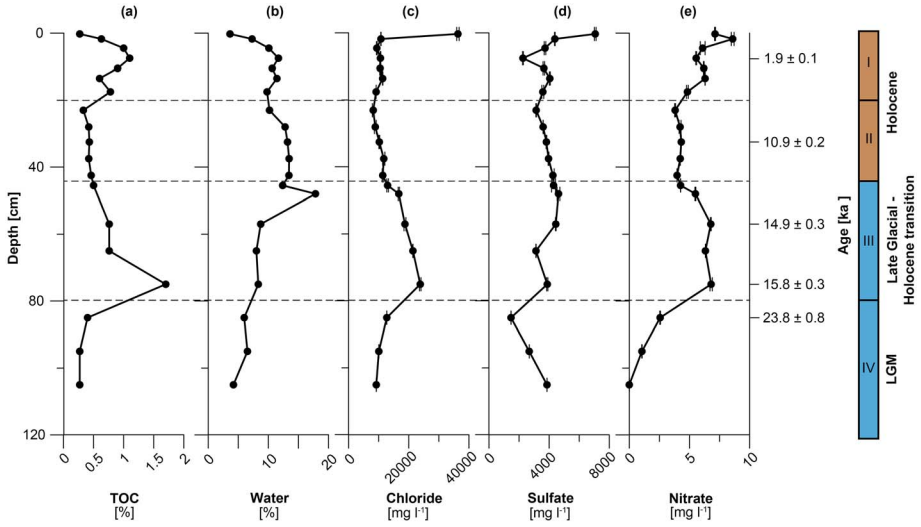

Figure 3. Abiotic and biotic parameters of Omongwa pan with depth. (a) Total organic carbon (wt %), (b) water content (%), (c) chloride (mg L^{-1}), (d) sulfate (mg L^{-1}), and (e) nitrate (L^{-1}); [c] to [e] obtained from sample leaching). Age data are provided by Schüller and Wehrmann (2016). An additional age date was obtained at 205 cm with 42.4 ± 0.8 ka (not shown). Standard deviations are indicated by a bar. Note different scales of *x* axis. LGM = Last Glacial Maximum.

conditions, and held for 16 min for equilibration. The flow rate was 200 µl min^{-1}, and injection was conducted by an autosampler (HTC PAL, CTC Analytic) with a 5 ml loop. APCI conditions were as follows: corona current of 5 µA (5 kV), a vaporizer temperature of 350°C, a capillary temperature of 200°C, and nitrogen sheath gas at 60 psi without auxiliary gas. The multiplier voltage was 1500 V, and the scan rate was 1 scan per second. Mass spectra were generated by selected ion monitoring in the positive ion mode using the following masses: for isoGDGTs m/z 1302, 1300, 1298, 1296, 1294, and 1292; for brGDGTs m/z 1050, 1048, 1046, 1036,1034, 1032, 1022, 1020, and 1018; and for archaeol 653. For semiquantitative determination of GDGT concentration an external synthetic archaeol standard was measured.

3. Results

3.1. Analysis of Sediment Properties

For better orientation during the result presentation and discussion Omongwa deposits are structured into four intervals according to age intervals and the separation of a near-surface interval. Interval I represents the near-surface interval comprising the top 20 cm. Interval II ranged from 45- to 20-cm depth. Both intervals were assigned to contain Holocene deposits. Interval III, spanning from 80 to 45 cm, covers the transition from the Last Glacial to Holocene period, and Interval IV ranged from 105- to 80-cm depth consisting of sediments from the LGM.

The sediment sequence was largely homogeneous over its 105-cm length. Medium to coarse silts together with dispersed evaporite crystals dominated the entire depth profile. Crystal layers were not observed. Overall, the TOC values ranged from 0.3 to 1.7 wt % with highest values in the top 20 cm (Interval I) and in Interval III with a maximum at 75-cm depth (Figure 3a). The water content in the upper layer was around 4% and increased to 18% at a depth of 50 cm. After this peak the water content decreased again with depth to 4% (Figure 3b). The most abundant anion was chloride (Cl^-) with concentrations from 8,200 to 36,300 mg L^{-1} (Figure 3c). Sulfate (SO_4^{2-}) concentrations were lower than Cl^- and ranged between 1,500 and 7,100 mg L^{-1} (Figure 3d). Both showed their highest amounts in samples close to the surface, followed by an abrupt decrease with depth. In the Holocene Interval II Cl^- and SO_4^{2-} were relatively constant. In Interval III Cl^- slightly increased with depth while SO_4^{2-} slightly decreased. In Interval IV Cl^- decreased again, whereas SO_4^{2-} concentration started to increase. Nitrate (NO_3^-) concentrations were significantly lower (up to 8.6 mg L^{-1}, Figure 3e) than Cl^- and SO_4^{2-}. Interval I and III showed highest amounts of NO_3^-. During Interval II a slight decrease was visible whereby Interval IV was characterized by a clear decline of NO_3^- (Figure 3e). The concentrations of small organic acids, such as acetate or formate were under the detection limit (< 0.2 mg L^{-1}) and could not be estimated.

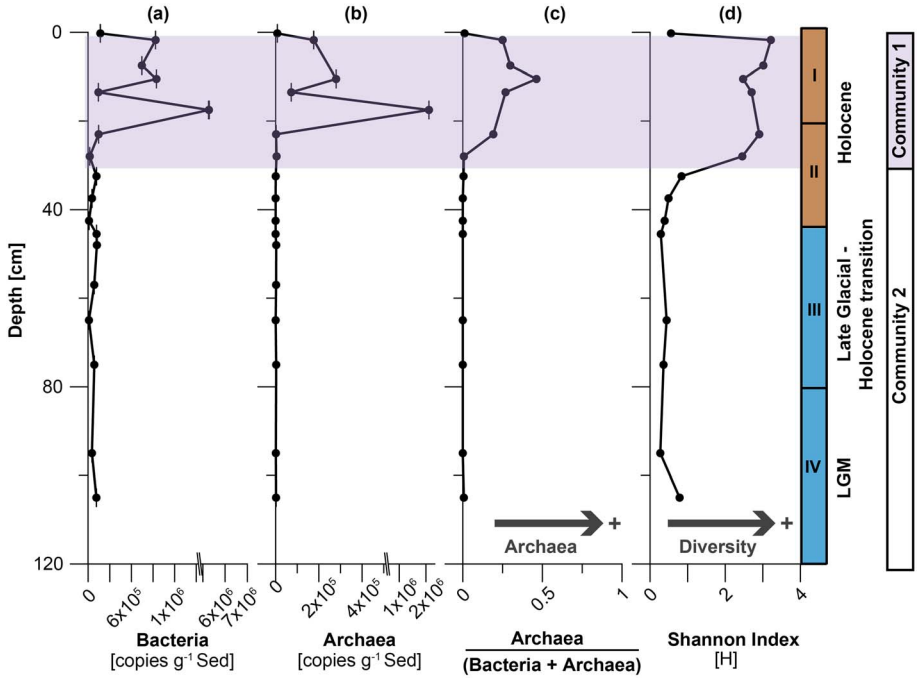

Figure 4. (a and b) qPCR results (a) abundance of bacterial small subunit ribonucleic acid genes (copies per gram sediment), (b) abundance of archaeal small subunit ribonucleic acid genes (copies per gram sediment), (c) Bacteria versus archaea based on operational taxonomic unit results (archaea/(bacteria + archaea), and (d) Shannon index (H) demonstrating the species diversity in a community based on sequencing data. The H index points to two different communities (C1 and C2; see also Figure 5). Standard deviations for qPCR data are indicated by a bar. LGM = Last Glacial Maximum.

3.2. Quantification of Bacterial and Archaeal Genes

Bacterial and archaeal SSU 16S rRNA gene copy numbers were highest in Interval I (uppermost 20 cm) with 6.1×10^6 bacterial copies per gram sediment (copies g^{-1} Sed) and 1.9×10^6 archaeal copies g^{-1} Sed (Figures 4a and 4b). Below the near-surface values decreased significantly with depth to 1.1×10^4 copies g^{-1} Sed for bacteria and 2.7×10^2 copies g^{-1} Sed for archaea. No copy numbers of archaea were calculated for samples between 35 and 47 cm due to the analytical detection limit.

3.3. Analyses of the Microbial Community Composition (NGS)

In the present study bacterial and archaeal phyla were detected by using high-throughput sequencing. After evaluating the internal standard (positive control), we decided to set a cutoff of 0.5% (minimum relative abundance of the OTU in the whole data set) to reduce the background noise which is typical for Illumina sequencing. In total, 131 OTUs were found. A ratio (archaea/archaea + bacteria) based on bacterial and archaeal OTUs was calculated (Figure 4c), showing a higher number of archaea within the top 23 cm (up to 48%). In total, 13 different phyla were detected (Figure 5).

Firmicutes dominate the depth profile of Omongwa pan from 30 to 105 cm as well as the surface layer (87–100%). All members of the phyla *Firmicutes* belonged to the families *Streptococcaceae* (3 OTUs, 0.7–34%), *Staphylococcaceae* (1 OTU, 1–5%), or *Bacillaceae* (7 OTUs, 4–100%). The overall majority of sequences assigned to *Firmicutes* showed highest similarity to *Bacillus*. A high proportion of *Euryarchaeota* (20–46%) and *Gemmatimonadetes* (22–60%) were found between 1 and 25 cm. *Proteobacteria* were dominating between 20 and 30 cm (25–48%). Furthermore, a high abundance of *Bacteroidetes* (2–14%) was observed between 1–20 cm and 30 cm. Almost all *Bacteroidetes* were attributed to the family *Rhodothermaceae* (8 OTUs). Thereby three of them were identified as *Salinibacter*. Furthermore, different phyla with less than 10% of relative abundance were found, such as *Actinobacteria* (7 OTUs), *Acidobacteria* (2 OTUs), *Chloroflexi* (1 OTU), *Cyanobacteria* (1 OTU), *Fusobacteria* (1 OTU), *Planctomycetes* (1 OTU), *Thermi* (1 OTU), candidate phylum *Acetothermia,* formerly known as OP1 (Nigro et al., 2016) (1 OTU), slight traces of *Crenarchaeota*

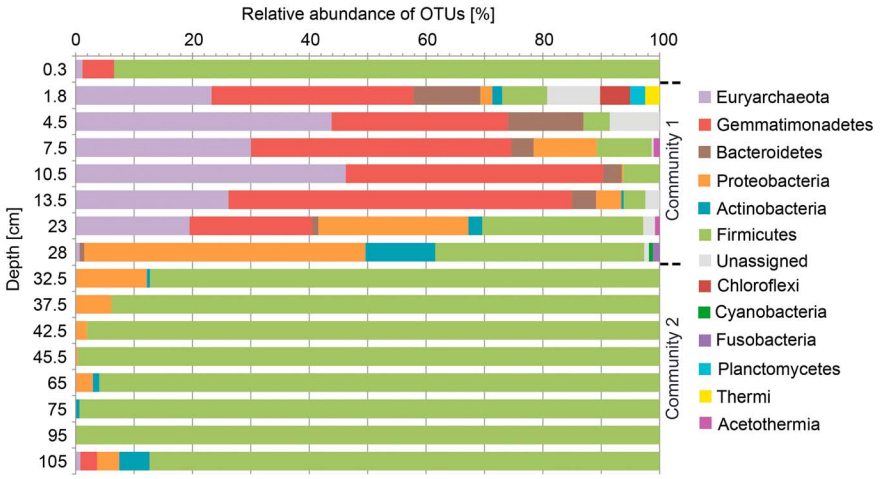

Figure 5. Diversity of the microbial community in Omongwa pan with depth showing the dominating bacterial and archaeal phyla by using high-throughput Illumina sequencing. OTUs = operational taxonomic units.

(1 OTU), and unassigned phyla (7 OTUs). Twenty-five archaeal OTUs were assigned to *Halobacteriaceae*. A few were identified on genus level (between 1 and 5 cm): *Natronomononas* (3 OTUs), *Natronococcus* (1 OTU), *Haloterrigena* (1 OTU), and *Halorhabdus* (2 OTUs).

The Shannon index (H) demonstrates the species diversity within a community (Colwell, 2009). Between 1.8 and 28 cm sediment depth the H index showed highest species diversity and varied from 2.4 to 3.2 (Figure 4d). At the surface and in the deeper layers the H index was significantly lower and ranged from 0.3 to 0.8. The PCA showed two main clusters indicating two different microbial communities within the core profile (Figure 6). The first factor explained 87% of the variance, whereas the second factor described 4% among all samples. Both communities displayed a distinct appearance, while community 1 (C1: from 1.8 to 28 cm depth) was mainly composed by taxonomically diverse groups, such as *Euryarchaeota, Gemmatimonadetes, Bacteroidetes, Chloroflexi, Plancomycetes*, and the candidate phylum *Acetothermia*. The second community (C2) was assigned to the uppermost sample (0.25 cm) and from 32 to 105 cm depth and mainly consisted of *Firmicutes*. The diversity of C2 was significantly lower than in C1 (Figure 4d). C1 showed a more diverse near-surface microbial community and was found in sediments of Holocene ages. In contrast C2 seems to represent the deeper microbial community in the pan sediments. The top layer of Omongwa pan (0.25 cm) was characterized by a salty crust and is different from C1 due to the dominance of *Firmicutes* and therefore resembles more the C2 community (Figure 6).

Statistical analysis based on OTU data (CCA) displayed six explanatory variables: chloride, fluoride, nitrate, TOC, and water content (Figure 7). The 41.3% of the total variance in bacterial and archaeal distribution was explained by these environmental parameters. Axis 1 explained 58.7% of the total variance, and axis 2 explained 22%.

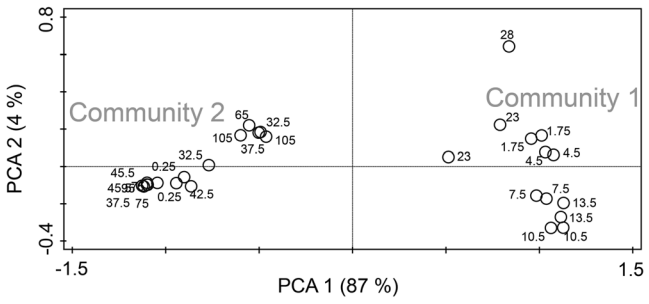

Figure 6. Principal component analyses (PCA) based on operational taxonomic unit sequencing data showing two distinct microbial communities (surface community C1 and deep community C2).

3.4. Depth Distribution of Present and Past Microbial Lipid Biomarkers

The detected PLFAs of Omongwa deposits can be divided into different groups, according to their chemical structures. Overall, saturated ($C_{12:0}$ to $C_{22:0}$), branched/saturated (*iso*-$C_{14:0}$, *iso/anteiso*-$C_{15:0}$, *iso*-$C_{16:0}$, *iso/ai*-$C_{17:0}$, $C_{10Me16:0}$), unsaturated ($C_{16:1\omega7c,t}$, $C_{16:1\omega5c,t}$, $C_{18:1\omega7c}$ and $C_{18:1\omega9}$, $C_{19:1br}$), and cyclo-$C_{17:1}$ PLFAs were identified. The highest amount of PLFAs was identified in Interval I in the uppermost samples from 0 to 3 cm sediment depth (up to 135 μg g^{-1} Sed). Below the surface layers concentrations decreased significantly with depth. In Interval II the lowest detection of PLFAs was observed (down to 3.6 μg

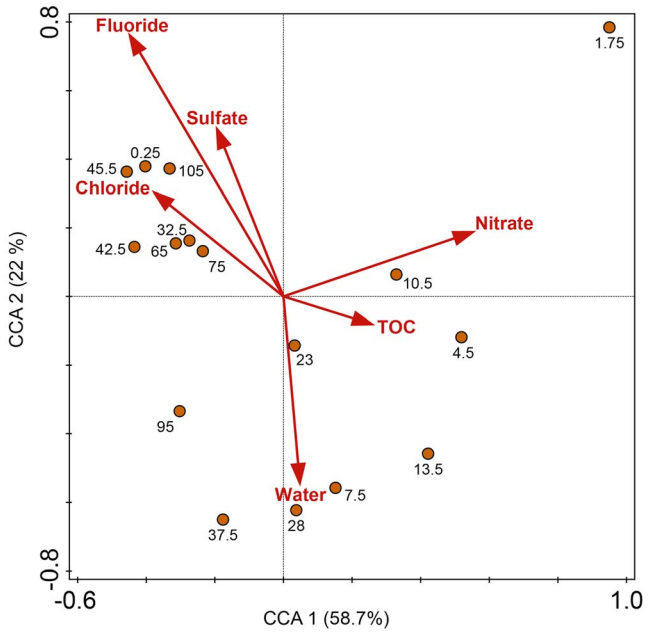

Figure 7. Canonical correspondence analysis (CCA) to determine relationship between environmental parameters and different sediment depth based on operational taxonomic unit sequencing data of Omongwa pan. Total variations were explained by 41.3% of the environmental parameter, whereby axis 1 (CCA 1) explained 58.7% and axis 2 (CCA 2) 22% of the total variance.

g^{-1} Sed, Figure 8a). In Interval III the PLFA signal slightly increased before the PLFA signal decreased again to low concentrations (2.4 μg g^{-1} Sed) in Interval IV.

Branched PLFAs occurred throughout the entire core. The *iso*- to *anteiso*-FA ratio ($iC_{15:0}$ + $iC_{17:0}$ / ($iC_{15:0}$ + $iC_{17:0}$) + ($aiC_{15:0}$ + $aiC_{17:0}$) indicated higher abundances of *iso*-FA in Intervals I and III (Figure 8b). Monounsaturated fatty acids like $C_{16:1\omega7c}$, $C_{18:1\omega7c}$, and $C_{18:1\omega9c}$ were dominant in the surface layers (0–3 cm depth, up to 64 μg g^{-1} Sed). Saturated PLFAs were analyzed within the entire core and they dominated the PLFA profile except for the top layers. The dominance of unsaturated fatty acids in the top layers and of saturated fatty acids in the deeper deposits is visualized by the ratio of saturated relative to unsaturated fatty acids ($C_{12:0}$ – $C_{22:0}$/($C_{12:0}$ – $C_{22:0}$) + ($C_{16:1\omega9}$, $C_{16:1\omega5}$ + $C_{16:1\omega7c}$ + $C_{18:1\omega7}$ + $C_{18:1\omega9}$)) in Figure 8c. The values of both ratios obtained for the top layers differed significantly from the rest of the profile.

brGDGTs were identified in the Omongwa samples representing typical soil bacterial biomarkers (Weijers et al., 2006). However, they were also reported to be produced in lake systems (Blaga et al., 2010). Bacterial brGDGTs (mainly composed of GDGT-I, GDGT-II, and GDGT-IIIa) ranging from 0 to 13.6 ng g^{-1} (for compound structures see Schouten et al., 2013). These biomarkers were more or less absent in Intervals I, II, and IV but show significant increase within Interval III (Figure 8d). At our study site established parameters to reconstruct pH and mean air temperature, like Cyclisation of Branched Tetraether and Methylation of Branched Tetraether ratios (Weijers

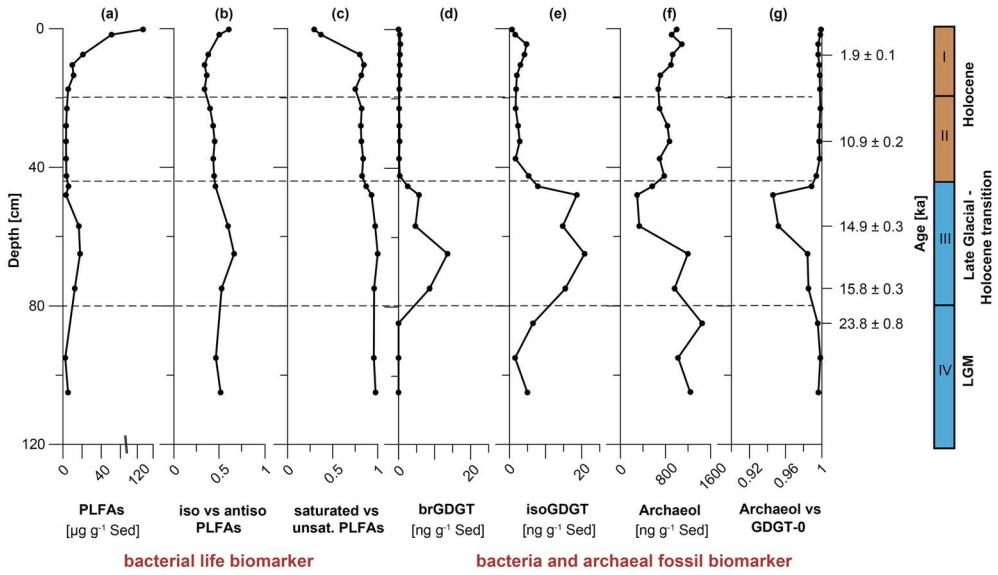

Figure 8. Depths profile of lipid microbial biomarkers. (a–c) bacterial life markers: (a) Concentration of all detected phospholipid derived fatty acids (PLFAs) in μg g^{-1} Sed, (b) ratio of *iso*- to *iso*- plus *anteiso*-PLFAs, and (c) ratio of saturated to saturated plus unsaturated PLFAs; (d–f) lipid biomarkers for the past microbial communities: (d) Concentration of bacterial branched glycerol dialkyl glycerol tetraethers (brGDGTs), (e) isoprenoid GDGT (isoGDGTs) and, (f) concentration of archaeol all in ng g^{-1} Sed, and (g) ratio of archaeol to archaeol plus isoGDGT-0. Age data provided by Schüller and Wehrmann (2016). Note different scales of *x* axis. LGM = Last Glacial Maximum.

et al., 2007), were not applicable due to the overall low abundance of brGDGTs, especially those with one or two additional cyclopentyl rings.

IsoGDGTs and archaeol were detected in the entire pan sediment profile and were used as characteristic markers for archaea (Schouten et al., 2013). The isoGDGT signal was composed of isoGDGT-0, isoGDGT-1, isoGDGT-2, and crenarchaeol, whereas isoGDGT-0 was the dominant compound. Total concentrations of isoGDGTs varied from 0.7 to 20.8 ng g^{-1} Sed (Figure 8e). Archaeol was present in significant concentrations at all depths and ranged from 296 to 1450 ng g^{-1} Sed. An increase of isoGDGT was measurable within Interval III coinciding with the increase of brGDGTs in the same interval. Archaeol showed higher abundances within Interval I (on average 884.8 ng g^{-1} Sed), coinciding with the higher detection of archaeal OTUs from *Halobacteriaceae* in the top layers (Figure 8f). The amount of archaeol decreased slightly and remained constant in Intervall II. A clear drop was observed in the top section of Interval III (on average 1079 ng g^{-1} Sed). In the lower section of Interval III archaeol concentration increased again and more or less stayed at this level down to Interval IV (on average 1162 ng g^{-1} Sed). The ratio between archaeol and isoGDGT-0 has been applied as a paleosalinity proxy for hypersaline systems due to the fact that halophilic *Euryarchaeota* mainly contains archaeol as membrane lipids (Turich & Freeman, 2011; Wang et al., 2013). Archaeol versus isoGDGT-0 ratio (Figure 8g) showed the strong dominance of archaeol in the entire sedimentary succession especially within Intervals I, II, and IV. In Interval III a relative shift to more isoGDGT-0 is indicated especially at the top section of this interval.

4. Discussion

4.1. Microbial Community Structure in Omongwa Pan Sediments

Aridity and the related saline and alkaline soil conditions have a large impact on microbial ecosystems (Shen et al., 2008) in saline pan sediments. Statistical analyses of NGS data revealed two distinct microbial communities in the depth profile of Omongwa pan (Figure 6) within distinct taxa diversity (Figure 4d). Community 1 (C1, 1.8 to 28 cm sediment depth) is characterized by a higher abundance (Figures 4a and 4b), a higher diversity of bacterial and archaeal sequences (Shannon index Ø 2.79, Figure 4d), and a specialized consortium of microorganisms, whereas community 2 (C2, 32.5 to 105 cm sediment depth) harvests only few species (Shannon index Ø 0.48, Figure 4d). Taxonomic similarity within Interval I suggests that DNA pools describe an abundant and more diverse surface microbial community (C1) which clearly can be distinguished from the deeper community (C2).

Metagenomic studies in arid areas show a higher prevalence of genes related to dormancy and stress response than in nonarid environments. This might be a consequence of evolutionary adjustment due to moisture and hot stress events (Fierer et al., 2012). Environmental factors such as water availability, salt content, and temperature conditions are important in explaining microbial community structure in desert environments (Angel & Conrad, 2013; Fierer et al., 2012; Garcia-Pichel et al., 2013; Stomeo et al., 2013). According to statistical analyses one factor basically determines the variance of the microbial community among pan samples (Figure 5). The PCA showed two distinct clusters of the microbial community along the *x* axis where occasional water availability might be the determining factor. The bioavailability of water is defined by evaporation and precipitation and also by the level of solutes in desert ground conditions (Pointing & Belnap, 2012). Occasional precipitation is infiltrating into the pan sediment influencing the microbial community C1.

Chloride moves conservatively in liquid water through the hydrologic cycle (Scanlon et al., 2009). Infiltrating precipitation caused Cl^- to move into or through the upper layers of the sediment and to accumulate at the surface by evaporation of the water. High concentrations of SO_4^{2-} as well as Cl^- in the top layers of Omongwa pan contribute to soil salinity (Oren, 2010; Scanlon et al., 2009) and might indicate restricted microbial activity under dry conditions. These pronounced saline conditions together with high ultraviolet (UV) radiation (Azua-Bustos et al., 2012; Meola et al., 2015) might have caused a different top layer community compared to the near-surface community C1 below. Due to the dominance of *Firmicutes,* namely, *Bacillus*, the top layer community is more similar to the deeper community C2 (Figures 5 and 6). The low water content in the surface sediments is probably one reason for seasonal microbial activity (Figure 3b). Further, environmental factors, like solar radiation, drought, temperature, and evaporation, may inhibit microbial growth in the top layer (Lange et al., 1998; Pen-Mouratov et al., 2011). Nitrate was measured in low concentration

(Figure 3e). It can be used as an electron acceptor for heterotrophic metabolism whereby buried organic matter is the most important carbon and energy source for organoheterotrophic microorganisms in sedimentary systems (Schaechter, 2009).

Euryarchaeota sequences related to *Halobacteriaceae* comprised 19 to 46% and were mainly detected in C1. *Halobacteriaceae* were only found in saline environments (Fendrihan et al., 2006; Montoya et al., 2013) and are known to dominate water bodies with sodium chloride concentration approaching saturation such as soda lakes or crystallizer ponds of solar salterns (Oren, 2002). The presence of extremely halophilic archaea was also observed in the near-surface layers of Witpan in the southwestern Kalahari (Genderjahn et al., 2017). Moreover, Lowenstein et al. (2011) showed that halophilic archaea trapped in fluid inclusions are able to survive desiccation over geologic time scales in hypersaline environments. These microorganisms are notably resistant to UV light while they are embedded in salt (Fendrihan et al., 2009; Jones & Baxter, 2017). In addition, *Halobacteriaceae* are known to balance osmotic pressure of the environment and resist the denaturing effects of salts (DasSarma & Arora, 2001) by accumulating several compatible solutes (e.g., sugars and amino acids) or inorganic ions (mainly potassium) in the cytoplasm (Oren, 2008). The negative charge of the cell surface is supposed to protect the proteins against denaturation, aggregation, and precipitation. Their proteins are either resistant to high salt concentrations or require salts for activity (DasSarma & Arora, 2001).

Gemmatimonadetes (clade divisions Gemm-2, Gemm-3, Gemm-4, and Gemm-5) were the dominant bacterial phyla in the upper 25 cm of Omongwa pan (Figure 5). *Gemmatimonadetes* are found in soil, marine, and lake sediments as well as in the Tataouine Desert of Tunisia (Chanal et al., 2006) and the hyperarid Atacama Desert in Chile (Drees et al., 2006). They seem to be more abundant in semiarid soils, suggesting that they are important colonists and perform well in adapting to low soil moisture (DeBruyn et al., 2011). *Gemmatimonadetes* have diverse metabolic capabilities to degrade high molecular weight organic matter, that is, proteins and carbohydrates (Thomas et al., 2011), suggesting the feasibility of decomposition of organic compounds in saline-alkaline soils.

Salinibacter is an extremely halophilic member of *Bacteroidetes*, belonging to the family *Rhodothermaceae*. Omongwa pan hosts significant communities of *Rhodothermaceae* in C1 together with the halophilic archaea of *Halobacteriaceae*, which require high salt concentration to grow (Anton et al., 2002). In desert ecosystems, where plants are usually rare, microorganisms are important for soil stability and soil productivity. The organisms are known to increase soil fertility (providing nutrients) and soil moisture retention (Pointing & Belnap, 2012) and thus influence the germination, survival, and nutritional status of the widely spaced vascular plants (Makhalanyane et al., 2015). *Actinobacteria* had been described as a dominant phylum in arid environments, such as the Namib Desert (Gunnigle et al., 2017; Makhalanyane et al., 2013). In Omongwa pan thermotolerant *Actinomycetales* (Kurapova et al., 2012) occured sporadically in C1 and C2. *Actinobacteria* are well adapted and have developed different strategies to survive, for example, sporulation, wide metabolic degradation capacity, synthesis of secondary metabolites, and various UV repair mechanisms (Ensign, 1978; Mccarthy & Williams, 1992). Several groups of *Proteobacteria* were found especially between 13.5 and 32.5 cm sediment depth. The most frequently found orders were *Rhizobiales, Burkhoderiales, Methylophilales*, and *Pseudomonadales. Proteobacteria* were often found in desert soil bacterial communities (Gunnigle et al., 2017; Lefevre et al., 2012; Spain et al., 2009) and may be functionally relevant in nutrient-limited arid environments (Boldareva-Nuianzina et al., 2013). We can summarize that near-surface layers of Omongwa pan are an important habitat for dry-adapted and halophilic bacteria as well as halophilic archaea. The C1 community shows a higher abundance and higher diversity.

In contrast, only a few phyla were detected in deeper successions (community C2). C2 was mainly composed of *Firmicutes* that play an important role in arid environments (Makhalanyane et al., 2015). The genus *Bacillus* predominanted the deeper layers (Figure 5) of Omongwa pan where the water content decreased compared to C1. Bacteria of the genus *Bacillus* are able to form endospores (Bertrand et al., 2015), which allow survival under extreme environmental conditions such as desiccation and high salt concentrations. In addition, synthesis and uptake of osmoprotectants such as compatible solutes (e.g., proline and glycine) or the import of potassium ions play an important role to survive in high-salinity environments (Schroeter et al., 2013). Sodium/proton antiporter are responsible to regulate the intracellular pH and enables *Bacillus* to survive in alkaline surroundings (Kitada et al., 1989).

4.2. Biomarker Signals of Living Microbial Communities

Studying community characteristics of such extreme saline and arid environments helps to estimate crucial factors of biodiversity development. Variations of the microbial community structure based on 16S rRNA gene high-throughput sequencing data are mainly attributed to differences in salinity (chloride and sulfate concentration) and water content (Figure 7), but so far, unspecified environmental parameters cannot be ruled out. The relatively increased numbers of bacterial and archaeal copy numbers (Figures 4a and 4b) might suggest a higher abundance of microorganisms within Interval I. However, PLFA life markers (Figure 8a) are only significantly increased in the top of Interval I and thus differ from the archaeal and bacterial signals obtained from cell copy numbers (Figures 4a and 4b). A reason for this discrepancy might be that the qPCR approach captures both intracellular DNA of intact cells and extracellular DNA as remnants from dead microorganisms. However, particularly high concentration of PLFAs life markers and higher gene copy numbers demonstrated the influence of near-surface processes on the microbial community in Omongwa pan. Occasionally or seasonally wetter conditions might stimulate a living microbial community in the top sediments. Near-surface microbial life might be activated by rainfall events providing biological resources such as water and nutrients into the pan system, which was already postulated for Witpan in the southern Kalahari (Genderjahn et al., 2017). Thus, temporally wet conditions affect the abundance and presumable activity of the actual surface microbial community. As Schirmack et al. (2015) described, microorganisms can desiccate and be inactive, but when water becomes available they can quickly hydrated and be active again. The PLFA signal indicated the presence of living bacteria, which could be active on a low metabolic level during dry periods and increase their activity during rainy season (December to February) when more water becomes available.

Variation in the total PLFA signal in sediments can either reflect changes in the microbial community composition and/or adaptation processes to external stress conditions. For instance, microorganisms are able to adapt to extreme temperature conditions by regulating the relative proportion of *iso* versus *anteiso* and saturated versus unsaturated fatty acids in their cell membranes. Warmer temperatures usually cause a shift to more saturated and *iso*-fatty acids (Kaneda, 1991; Rilfors et al., 1978; Russell, 1989). In our study the fatty acid ratios showed a trend to more *iso*- and unsaturated fatty acids in the upper layers (Interval I) being exposed to the hot desert conditions (Figures 8b and 8c). The same trend was demonstrated in Witpan in the southwestern Kalahari (Genderjahn et al., 2017). While the *iso* versus *anteiso* ratio might resemble temperature adaptation, the saturated versus unsaturated ratio rather reflects variations in the overall microbial community regarding to the harsh conditions and nutrient stress (Bach et al., 2010). The surface layer is mainly determined by monounsaturated PLFAs and differs significantly from those below. Gram-negative bacteria contain a large proportion of monounsaturated fatty acids (Piotrowska-Seget & Mrozik, 2003; Zelles, 1999). Literature reports point out that the content of these compounds increases with salt concentration which refers to an increase of gram-negative halophilic bacteria (Ventosa et al., 1998). This is also supported by our community data of Omongwa pan, which indicated higher abundance of gram-negative *Gemmatimonadete*s and gram-negative *Bacteroidetes* in C1.

4.3. Insights Into Paleoenvironmental Conditions Using Past Microbial Lipid Biomarkers

In contrast to PLFA biomarkers, archaeol and GDGTs reflect dead or past microbial biomass and are therefore often used to trace remnants of ancient microbial communities in older sediments (Schouten et al., 2013). However, in sedimentary depth intervals with an increased microbial life these biomarkers also could represent degradation products of actual living microorganisms. To distinguish between these two cases, the abundance of past markers was compared with the PLFA life marker depth profile. In the current study PLFA life markers are only dominant in the surface layers (Figure 8a). Thus, for Interval I GDGTs and archaeol are not unambiguously applicable to trace past microbial communities. Compared to Interval I, there is only low microbial life indicated in the deeper sedimentary succession by the PLFAs. Additionally, bacterial and archaeal DNA are not very abundant below the surface Interval I (Figures 4a and 4b) providing no indication for increased microbial life in deeper successions. Therefore, in the deeper pan deposits GDGTs and archaeol resembled molecular remains of past microbial communities. Furthermore, it has to be mentioned that brGDGTs only represent a small part of the total bacterial community different from those providing for instance cell membrane PL esters. Bacteria containing brGDGTs are often interpreted as soil bacteria (Weijers et al., 2007). Thus, these biomarkers can be used to trace variations of specific bacteria from soils

with depth but provide no information on the total abundance of past bacterial communities. Moreover, brGDGTs can also be produced in freshwater systems (De Jonge et al., 2014). Since Omongwa pan might have allowed standing water for longer periods of time in the past this origin cannot be ruled out completely. In contrast to brGDGTs, archaeol and isoGDGTs are membrane markers representing the whole past archaeal communities. Genderjahn et al. (2017) could show that the archaeol and GDGT core lipids are presumably less affected by post depositional degradation and that their concentrations essentially reflect compound production in the past. Another argument, that in deeper pan successions archaeol and GDGTs represent past microbial communities from time of deposition, is our results concerning the modern microbial community structure of Omongwa pan. The data show that abundant microbial life seems to be related to the surface and that intensive life in the deeper parts are restricted. In surface layers (Interval I) the elemental parameters and biomarker data might be complicated by an active system of organic matter production, degradation, and deposition associated to an actual living and active microbial community. Thus, organic matter (TOC) still undergoes severe depositional transformation, especially since in an arid environment recycling and remineralization might be an important process. The presence of life markers and the higher microbial diversity strongly point to at least occasional rainfall in this area.

The brGDGT and isoGDGT profiles (Figures 8d and 8e) as well as the TOC data are markedly increased in Interval III, suggesting a larger abundance of past microorganisms. In contrast, the archaeol signal (Figure 8f) is significantly decreased during the upper section of Interval III (Figures 8f and 8g). Halophilic archaea mainly produce archaeol and not isoGDGT-0 (Schouten et al., 2013). For this reason the relative abundance of archaeol and isoGDGT-0 can be used as a paleosalinity proxy for hypersaline environments due to the predominance of halophilic *Euryarchaeota* (Turich & Freeman, 2011; Wang et al., 2013). Sequencing analyses support the assumption that archaeol is mainly produced by *Halobacteria* due to the absence of OTUs of different archaeol-producing archaea such as methanogens. At Omongwa pan archaeol is dominating the archaeol versus isoGDGT-0 ratio in Holocene Intervals I, II, and LGM Interval IV (Figure 8f) indicating strong halophilic and presumably dry conditions in an arid environment. In contrast, the lower ratio values especially in the upper sediments of Interval III can be interpreted as a shift toward a less halophilic archaeal community in the pan system reflecting a period of somewhat higher paleoprecipitation at the Late Glacial to Holocene transition. Higher paleoprecipitation is supported by the increase in brGDGT soil biomarkers during Interval III (Figure 8d) indicating higher supply of soil organic matter from the catchment area into the pan during this period (or production of brGDGTs in longer standing water). Additionally, much higher sedimentation rates are indicated by the age data (Schüller & Wehrmann, 2016) promoting a scenario of higher paleoprecipitation during Interval III. Finally, higher TOC indicates stimulation of organic matter production and transport into the pan during this time period.

The increase of archaeal isoGDGTs in Interval III is not resembled by a stronger archaeal proportion in the community C2 (Figure 5) supporting that GDGTs indeed represent a past microbial signal and vice versa that the DNA presumably represents predominantly a modern microbial community. Thus, the biomarker data indicate that during the LGM (Interval IV) stronger halophilic and therefore dryer conditions prevailed in the western Kalahari. In contrast, at the Late Glacial to Holocene transition (Interval III) conditions seem to change to a scenario with increased paleoprecipitation. During the Holocene aridity increased again due to higher temperatures and stronger global circulation systems, and consequently reducing both wind strength and the influence of moisture in the Omongwa area (Chase & Thomas, 2006; Gasse et al., 2008).

The study of Genderjahn et al. (2017) and Telfer et al. (2009) at Witpan in the southwestern Kalahari indicated a period of increased paleoprecipitation during the LGM that is in accordance with a northeast shift of the winter rainfall zone observed in southwestern Africa during the LGM (Chase & Meadows, 2007). This movement was caused by the northward migration of the westerlies in consequence of the Antarctic sea ice expansion during this period (Sime et al., 2013). However, comparing both studies, the northeast extension of the winter rainfall zone during the LGM did not affect the Omongwa region in the western Kalahari. In contrast, biomarker analyses of Omongwa pan suggested dry conditions in the western Kalahari during the LGM and a later paleoclimatic change to wetter conditions during the Late Glacial to Holocene transition period, which was in return not observed in the Witpan deposits. This indicates that the paleoprecipitation in the western Kalahari was influenced from the northeast. A conceivable scenario for this region could be that in response to the southwest retreat of the winter rainfall zone during the deglaciation the ITCZ, driven by

strong trade winds, shifted more to the southwest. Strong trade winds transporting rain from the Indian Ocean could have led to intensified summer rainfall in the western Kalahari during the transition from the Last Glacial to the Holocene. A southward shift of the ITCZ was postulated by Schefuss et al. (2011) during the Heinrich Stadial I (ca. 18–14.8 ka). Our results might indicate that the movement of the ITCZ also affected precipitation in the Kalahari region. However, this movement did not affect the southwestern Kalahari at Witpan. The biomarker depth profiles of two different Kalahari pans suggested that the Holocene was drier compared to the Last Glacial to Holocene transition (Genderjahn et al., 2017). During the Holocene reduced wind strength might have caused an easterly retreat of the main summer rainfall zone (Gasse et al., 2008) leading again to semiarid to arid conditions in the Kalahari region. In accordance, a marine record in front of the Namibian coastline pointed out dryer conditions during the early and mid-Holocene (Collins et al., 2014). Subsequently, Collins et al. (2014) addressed these changes to enhanced eastern African monsoon due to maximum of a Southern Hemisphere summer insolation.

5. Conclusion

Analyses of the microbial community by means of NGS and biomarker data disclose deep insights into microbial pan communities and past environmental variations in the western Kalahari. Due to high evaporation and desiccation of surface waters aridification is constantly progressing in the Kalahari region. Surface processes play a central role for the modern microbial pan communities and determine the microbial composition in the top layers. The presence of life markers showed the occurrence of living bacterial communities in Omongwa pan mainly in the topmost deposits. In the near-surface sediments higher species diversity was observed compared to deeper layers presumably as the result of occasional water and nutrient provision to the surface layers. The microbial community in Omongwa pan was characterized by a high relative abundance (up to 48%) of halophilic archaea (*Halobacteriaceae*). Observed bacterial taxa are likewise halophilic (e.g., *Salinibacter* and *Sainisaeta*), known to be well adapted to the semiarid conditions (e.g., *Gemmatimonadetes*) and elevated temperatures (e.g., *Actinomycetales* and *Rhodothermacea*).

Lipid biomarkers for past microbial communities indicated significant response of microbial ecosystems with respect to paleoclimate variations. The northeastern extension of the winter rainfall zone during the LGM observed in Witpan deposits in the southwestern Kalahari (Genderjahn et al., 2017) was not detected in Omongwa pan sediments in the western Kalahari. Instead, a period of increased paleoprecipitation in the western Kalahari was indicated during the Late Glacial to Holocene transition. This was possibly caused by a southwestern shift in the position of the summer rainfall zone associated to the southward movement of the ITCZ. The Omongwa pan study confirms, in addition to the Witpan study, the potential of continental pans to act as geoarchives for characteristic biomolecules reflecting paleoclimate information.

Acknowledgments
We thank the Namibian Geological Survey for logistic and administrative support. Special thanks to Fabian Horn (German Research Centre for Geosciences-Helmholtz Centre Potsdam, GFZ) and his bioinformatics expertise. Thanks go to Robert Milewski (GFZ) for providing the aerial image. Thanks for technical assistance and help of Anke Kaminski, Cornelia Karger, Kristin Günther, and Jakob Wiese (all GFZ). We are also grateful to the reviewers of JGR Biogeosciences and the Editor Ankur Desai for their helpful and constructive comments. We thank all GeoArchives project partners. The project "Signals of climate and landscape change preserved in southern African GeoArchives" (project 03G0838B/C) is part of the SPACES program (Science Partnerships for the Assessment of Complex Earth System Processes), which is financially supported by the German Federal Ministry of Education and Research (BMBF). Data on grain sizes (Schüller & Wehrmann, 2017) and age determinations (Schüller & Wehrmann, 2016) of Omongwa pan were archived in PANGAEA database. Nucleotide sequencing information were deposited at the European Nucleotide Archive (sample accession: ERS1599441–ERS1599469). All other data are compiled in tables and added as supporting information.

References

Ahrens, C. D., & Samson, P. J. (2010). *Extreme weather and climate*. Belmont, CA: Brooks/Cole, Cengage Learning.

Angel, R., & Conrad, R. (2013). Elucidating the microbial resuscitation cascade in biological soil crusts following a simulated rain event. *Environmental Microbiology*, *15*(10), 2799–2815. https://doi.org/10.1111/1462-2920.12140

Anton, J., Oren, A., Benlloch, S., Rodriguez-Valera, F., Amann, R., & Rossello-Mora, R. (2002). *Salinibacter ruber* gen. nov., sp. nov., a novel, extremely halophilic member of the Bacteria from saltern crystallizer ponds. *International Journal of Systematic and Evolutionary Microbiology*, *52*(2), 485–491. https://doi.org/10.1099/00207713-52-2-485

Azua-Bustos, A., Urrejola, C., & Vicuna, R. (2012). Life at the dry edge: Microorganisms of the Atacama Desert. *FEBS Letters*, *586*(18), 2939–2945. https://doi.org/10.1016/j.febslet.2012.07.025

Bach, E. M., Baer, S. G., Meyer, C. K., & Six, J. (2010). Soil texture affects soil microbial and structural recovery during grassland restoration. *Soil Biology & Biochemistry*, *42*(12), 2182–2191. https://doi.org/10.1016/j.soilbio.2010.08.014

Baker, G. C., Smith, J. J., & Cowan, D. A. (2003). Review and re-analysis of domain-specific 16s primers. *Journal of Microbiological Methods*, *55*(3), 541–555.

Benison, K. C., & Karmanocky, F. J. (2014). Could microorganisms be preserved in Mars gypsum? Insights from terrestrial examples. *Geology*, *42*(7), 615–618. https://doi.org/10.1130/g35542.1

Bertrand, J. C., Caumette, P., Lebaron, P., Matheron, R., Normand, P., & Sime-Ngando, T. (2015). *Environmental microbiology: Fundamentals and applications: Microbial ecology*. Dordrecht, Netherlands: Springer.

Blaga, C. I., Reichart, G. J., Heiri, O., & Damste, J. S. S. (2009). Tetraether membrane lipid distributions in water-column particulate matter and sediments: A study of 47 European lakes along a north-south transect. *Journal of Paleolimnology*, *41*(3), 523–540. https://doi.org/10.1007/s10933-008-9242-2

Blaga, C. I., Reichart, G.-J., Schouten, S., Lotter, A. F., Werne, J. P., Kosten, S., et al. (2010). Branched glycerol dialkyl glycerol tetraethers in lake sediments: Can they be used as temperature and pH proxies? *Organic Geochemistry*, *41*(11), 1225–1234. https://doi.org/10.1016/j.orggeochem.2010.07.002

Bligh, E. G., & Dyer, W. J. (1959). A rapid method of total lipid extraction and purification. *Canadian Journal of Biochemistry and Physiology*, *37*(8), 911–917. https://doi.org/10.1139/o59-099

Blume, H. P., Stahr, K., & Leinweber, P. (2011). Bodenkundliches Praktikum: Eine Einführung in pedologisches Arbeiten für Ökologen, Land- und Forstwirte. In *Geo- und Umweltwissenschaftler* (Chapter 5.3.1). Heidelberg: Spektrum Akademischer Verlag.

Boldareva-Nuianzina, E. N., Blahova, Z., Sobotka, R., & Koblizek, M. (2013). Distribution and origin of oxygen-dependent and oxygen-independent forms of Mg-protoporphyrin monomethylester cyclase among phototrophic proteobacteria. *Applied and Environmental Microbiology*, *79*(8), 2596–2604. https://doi.org/10.1128/AEM.00104-13

Bolger, A. M., Lohse, M., & Usadel, B. (2014). Trimmomatic: A flexible trimmer for Illumina sequence data. *Bioinformatics*, *30*(15), 2114–2120. https://doi.org/10.1093/bioinformatics/btu170

Butzer, K. W., Stuckenrath, R., Bruzewicz, A. J., & Helgren, D. M. (2017). Late Cenozoic paleoclimates of the Gaap Escarpment, Kalahari margin, South Africa. *Quaternary Research*, *10*(03), 310–339. https://doi.org/10.1016/0033-5894(78)90025-x

Caporaso, J. G., Kuczynski, J., Stombaugh, J., Bittinger, K., Bushman, F. D., Costello, E. K., et al. (2010). QIIME allows analysis of high-throughput community sequencing data. *Nature Methods*, *7*(5), 335–336. https://doi.org/10.1038/nmeth.f.303

Caporaso, J. G., Lauber, C. L., Walters, W. A., Berg-Lyons, D., Lozupone, C. A., Turnbaugh, P. J., et al. (2011). Global patterns of 16S rRNA diversity at a depth of millions of sequences per sample. *Proceedings of the National Academy of Sciences of the United States of America*, *108*(Supplement_1), 4516–4522. https://doi.org/10.1073/pnas.1000080107

Chanal, A., Chapon, V., Benzerara, K., Barakat, M., Christen, R., Achouak, W., et al. (2006). The desert of Tataouine: An extreme environment that hosts a wide diversity of microorganisms and radiotolerant bacteria. *Environmental Microbiology*, *8*(3), 514–525. https://doi.org/10.1111/j.1462-2920.2005.00921.x

Chase, B. M., Boom, A., Carr, A. S., Meadows, M. E., & Reimer, P. J. (2013). Holocene climate change in southernmost South Africa: Rock hyrax middens record shifts in the southern westerlies. *Quaternary Science Reviews*, *82*, 199–205. https://doi.org/10.1016/j.quascirev.2013.10.018

Chase, B. M., & Meadows, M. E. (2007). Late quaternary dynamics of southern Africa's winter rainfall zone. *Earth-Science Reviews*, *84*(3–4), 103–138. https://doi.org/10.1016/j.earscirev.2007.06.002

Chase, B. M., & Thomas, D. S. G. (2006). Late Quaternary dune accumulation along the western margin of South Africa: Distinguishing forcing mechanisms through the analysis of migratory dune forms. *Earth and Planetary Science Letters*, *251*(3–4), 318–333. https://doi.org/10.1016/j.epsl.2006.09.017

Collins, J. A., Schefuss, E., Govin, A., Mulitza, S., & Tiedemann, R. (2014). Insolation and glacial-interglacial control on southwestern African hydroclimate over the past 140 000 years. *Earth and Planetary Science Letters*, *398*, 1–10. https://doi.org/10.1016/j.epsl.2014.04.034

Colwell, R. K. (2009). Biodiversity: Concepts, patterns and measurement. In S. A. Levin (Ed.), *The Princeton guide to ecology* (pp. 257–263). Princeton, NJ: Princeton University Press.

Coolen, M. J., & Gibson, J. A. (2009). Ancient DNA in lake sediment records. *PAGES News*, *17*(3), 104–106. https://doi.org/10.22498/pages.17.3.104

DasSarma, S., & Arora, P. (2001). *Halophiles eLS*. Chichester, UK: John Wiley.

De Jonge, C., Stadnitskaia, A., Hopmans, E. C., Cherkashov, G., Fedotov, A., & Sinninghe Damsté, J. S. (2014). In situ produced branched glycerol dialkyl glycerol tetraethers in suspended particulate matter from the Yenisei River, Eastern Siberia. *Geochimica et Cosmochimica Acta*, *125*, 476–491. https://doi.org/10.1016/j.gca.2013.10.031

DeBruyn, J. M., Nixon, L. T., Fawaz, M. N., Johnson, A. M., & Radosevich, M. (2011). Global biogeography and quantitative seasonal dynamics of Gemmatimonadetes in soil. *Applied and Environmental Microbiology*, *77*(17), 6295–6300. https://doi.org/10.1128/AEM.05005-11

Drees, K. P., Neilson, J. W., Betancourt, J. L., Quade, J., Henderson, D. A., Pryor, B. M., & Maier, R. M. (2006). Bacterial community structure in the hyperarid core of the Atacama Desert, Chile. *Applied and Environmental Microbiology*, *72*(12), 7902–7908. https://doi.org/10.1128/AEM.01305-06

Ensign, J. C. (1978). Formation, properties, and germination of actinomycete spores. *Annual Review of Microbiology*, *32*(1), 185–219. https://doi.org/10.1146/annurev.mi.32.100178.001153

Fendrihan, S., Berces, A., Lammer, H., Musso, M., Ronto, G., Polacsek, T. K., et al. (2009). Investigating the effects of simulated Martian ultraviolet radiation on *Halococcus dombrowskii* and other extremely halophilic archaebacteria. *Astrobiology*, *9*(1), 104–112. https://doi.org/10.1089/ast.2007.0234

Fendrihan, S., Legat, A., Pfaffenhuemer, M., Gruber, C., Weidler, G., Gerbl, F., & Stan-Lotter, H. (2006). Extremely halophilic archaea and the issue of long-term microbial survival. *Reviews in Environmental Science and Biotechnology*, *5*(2–3), 203–218. https://doi.org/10.1007/s11157-006-0007-y

Fierer, N., Leff, J. W., Adams, B. J., Nielsen, U. N., Bates, S. T., Lauber, C. L., et al. (2012). Cross-biome metagenomic analyses of soil microbial communities and their functional attributes. *Proceedings of the National Academy of Sciences of the United States of America*, *109*(52), 21,390–21,395. https://doi.org/10.1073/pnas.1215210110

Garcia-Pichel, F., Loza, V., Marusenko, Y., Mateo, P., & Potrafka, R. M. (2013). Temperature drives the continental-scale distribution of key microbes in topsoil communities. *Science*, *340*(6140), 1574–1577. https://doi.org/10.1126/science.1236404

Gasse, F., Chalie, F., Vincens, A., Williams, M. A. J., & Williamson, D. (2008). Climatic patterns in equatorial and southern Africa from 30,000 to 10,000 years ago reconstructed from terrestrial and near-shore proxy data. *Quaternary Science Reviews*, *27*(25–26), 2316–2340. https://doi.org/10.1016/j.quascirev.2008.08.027

Genderjahn, S., Alawi, M., Kallmeyer, J., Belz, L., Wagner, D., & Mangelsdorf, K. (2017). Present and past microbial life in continental pan sediments and its response to climate variability in the southern Kalahari. *Organic Geochemistry*, *108*, 30–42. https://doi.org/10.1016/j.orggeochem.2017.04.001

Goudie, A. S., & Thomas, D. S. G. (1985). Pans in southern Africa with particular reference to South Africa and Zimbabwe. *Zeitschrift für Geomorphologie*, *01*(29), 1–19.

Goudie, A. S., & Wells, G. L. (1995). The nature, distribution and formation of pans in arid zones. *Earth-Science Reviews*, *38*(1), 1–69. https://doi.org/10.1016/0012-8252(94)00066-6

Gunnigle, E., Frossard, A., Ramond, J. B., Guerrero, L., Seely, M., & Cowan, D. A. (2017). Diel-scale temporal dynamics recorded for bacterial groups in Namib Desert soil. *Scientific Reports*, *7*, 40189. https://doi.org/10.1038/srep40189

Heine, K. (2004). Flood reconstructions in the Namib Desert, Namibia and Little Ice Age climatic implications: Evidence from slackwater deposits and desert soil sequences. *Journal of the Geological Society of India*, *64*(4), 535–547.

Heine, K. (2005). Holocene climate of Namibia: A review based geoarchives. *African Study Monographs* (Suppl. 30, pp. 119–133). Kyoto.

Holmgren, K., & Shaw, P. (1997). Palaeoenvironmental reconstruction from near-surface pan sediments: An example from Lebatse Pan, southeast Kalahari, Botswana. *Geografiska Annaler Series a-Physical Geography*, *79A*(1–2), 83–93. https://doi.org/10.1111/1468-0459.00008

Hopmans, E. C., Schouten, S., Pancost, R. D., van der Meer, M. T., & Sinninghe Damste, J. S. (2000). Analysis of intact tetraether lipids in archaeal cell material and sediments by high performance liquid chromatography/atmospheric pressure chemical ionization mass spectrometry. *Rapid Communications in Mass Spectrometry*, *14*(7), 585–589. https://doi.org/10.1002/(SICI)1097-0231(20000415)14:7<585::AID-RCM913>3.0.CO;2-N

Jiang, H., Dong, H., Zhang, G., Yu, B., Chapman, L. R., & Fields, M. W. (2006). Microbial diversity in water and sediment of Lake Chaka, an athalassohaline lake in northwestern China. *Applied and Environmental Microbiology*, *72*(6), 3832–3845. https://doi.org/10.1128/AEM.02869-05

Johnson, S. S., Chevrette, M. G., Ehlmann, B. L., & Benison, K. C. (2015). Insights from the metagenome of an acid salt lake: The role of biology in an extreme depositional environment. *PLoS One*, *10*(4), e0122869. https://doi.org/10.1371/journal.pone.0122869

Jones, D. L., & Baxter, B. K. (2017). DNA repair and photoprotection: Mechanisms of overcoming environmental ultraviolet radiation exposure in halophilic archaea. *Frontiers in Microbiology*, *8*, 1882. https://doi.org/10.3389/fmicb.2017.01882

Kaneda, T. (1991). Iso-fatty and Anteiso-fatty acids in bacteria—Biosynthesis, function, and taxonomic significance. *Microbiological Reviews*, *55*(2), 288–302.

Kates, M. (1996). Structural analysis of phospholipids and glycolipids in extremely halophilic archaebacteria. *Journal of Microbiological Methods*, *25*(2), 113–128. https://doi.org/10.1016/0167-7012(96)00010-3

Kitada, M., Onda, K., & Horikoshi, K. (1989). The sodium/proton antiport system in a newly isolated alkalophilic *Bacillus* sp. *Journal of Bacteriology*, *171*(4), 1879–1884. https://doi.org/10.1128/jb.171.4.1879-1884.1989

Kurapova, A. I., Zenova, G. M., Sudnitsyn, I. I., Kizilova, A. K., Manucharova, N. A., Norovsuren, Z., & Zvyagintsev, D. G. (2012). Thermotolerant and thermophilic actinomycetes from soils of Mongolia Desert steppe zone. *Microbiology*, *81*(1), 98–108. https://doi.org/10.1134/S0026261712010092

Kysela, D. T., Palacios, C., & Sogin, M. L. (2005). Serial analysis of V6 ribosomal sequence tags (SARST-V6): A method for efficient, high-throughput analysis of microbial community composition. *Environmental Microbiology*, *7*(3), 356–364. https://doi.org/10.1111/j.1462-2920.2004.00712.x

Lancaster, I. N. (1976). *The pans of the southern Kalahari, Botswana* (pp. 59–67). Cambridge: University of Cambridge.

Lancaster, I. N. (1986). Pans in the southwestern Kalahari: A preliminary report. *Palaeoecology of Africa*, *17*(5).

Lange, O. L., Belnap, J., & Reichenberger, H. (1998). Photosynthesis of the cyanobacterial soil-crust lichen *Collema tenax* from arid lands in southern Utah, USA: Role of water content on light and temperature responses of CO(2) exchange. *Functional Ecology*, *12*(2), 195–202. https://doi.org/10.1046/j.1365-2435.1998.00192.x

Lefevre, C. T., Viloria, N., Schmidt, M. L., Posfai, M., Frankel, R. B., & Bazylinski, D. A. (2012). Novel magnetite-producing magnetotactic bacteria belonging to the Gammaproteobacteria. *The ISME Journal*, *6*(2), 440–450. https://doi.org/10.1038/ismej.2011.97

Logemann, J., Graue, J., Koster, J., Engelen, B., Rullkotter, J., & Cypionka, H. (2011). A laboratory experiment of intact polar lipid degradation in sandy sediments. *Biogeosciences*, *8*(9), 2547–2560. https://doi.org/10.5194/bg-8-2547-2011

Lowenstein, T. K., & Hardie, L. A. (1985). Criteria for the recognition of salt-pan evaporites. *Sedimentology*, *32*(5), 627–644. https://doi.org/10.1111/j.1365-3091.1985.tb00478.x

Lowenstein, T. K., Schubert, B. A., & Timofeeff, M. N. (2011). Microbial communities in fluid inclusions and long-term survival in halite. *GSA Today*, *21*(1), 4–9. https://doi.org/10.1130/GSATG81A.1

Makhalanyane, T. P., Valverde, A., Gunnigle, E., Frossard, A., Ramond, J. B., & Cowan, D. A. (2015). Microbial ecology of hot desert edaphic systems. *FEMS Microbiology Reviews*, *39*(2), 203–221. https://doi.org/10.1093/femsre/fuu011

Makhalanyane, T. P., Valverde, A., Lacap, D. C., Pointing, S. B., Tuffin, M. I., & Cowan, D. A. (2013). Evidence of species recruitment and development of hot desert hypolithic communities. *Environmental Microbiology Reports*, *5*(2), 219–224. https://doi.org/10.1111/1758-2229.12003

Maturrano, L., Santos, F., Rossello-Mora, R., & Anton, J. (2006). Microbial diversity in Maras salterns, a hypersaline environment in the Peruvian Andes. *Applied and Environmental Microbiology*, *72*(6), 3887–3895. https://doi.org/10.1128/AEM.02214-05

Mccarthy, A. J., & Williams, S. T. (1992). Actinomycetes as agents of biodegradation in the environment—A review. *Gene*, *115*(1-2), 189–192. https://doi.org/10.1016/0378-1119(92)90558-7

Mees, F. (1999). Distribution patterns of gypsum and kalistrontite in a dry lake basin of the southwestern Kalahari (Omongwa pan, Namibia). *Earth Surface Processes and Landforms*, *24*(8), 731–744. https://doi.org/10.1002/(SICI)1096-9837(199908)24:8<731::AID-ESP7>3.0.CO;2-0

Meola, M., Lazzaro, A., & Zeyer, J. (2015). Bacterial composition and survival on Sahara dust particles transported to the European Alps. *Frontiers in Microbiology*, *6*, 1454. https://doi.org/10.3389/fmicb.2015.01454

Milewski, R., Chabrillat, S., & Behling, R. (2017). Analyses of recent sediment surface dynamic of a Namibian Kalahari salt pan based on multitemporal Landsat and hyperspectral hyperion data. *Remote Sensing*, *9*, 170. https://doi.org/10.3390/Rs9020170

Montoya, L., Vizioli, C., Rodriguez, N., Rastoll, M. J., Amils, R., & Marin, I. (2013). Microbial community composition of Tirez lagoon (Spain), a highly sulfated athalassohaline environment. *Aquatic Biosystems*, *9*(1), 19. https://doi.org/10.1186/2046-9063-9-19

Müller, K. D., Husmann, H., & Nalik, H. P. (1990). A new and rapid method for the assay of bacterial fatty-acids using high-resolution capillary gas-chromatography and trimethylsulfonium hydroxide. *Zentralblatt Fur Bakteriologie-International Journal of Medical Microbiology Virology Parasitology and Infectious Diseases*, *274*(2), 174–182.

Nadkarni, M. A., Martin, F. E., Jacques, N. A., & Hunter, N. (2002). Determination of bacterial load by real-time PCR using a broad-range (universal) probe and primers set. *Microbiology-Sgm*, *148*, 257–266. https://doi.org/10.1099/00221287-148-1-257

Nash, D. J., & McLaren, S. J. (2003). Kalahari valley calcretes: Their nature, origins, and environmental significance. *Quaternary International*, *111*(1), 3–22. https://doi.org/10.1016/S1040-6182(03)00011-9

Nigro, L. M., Hyde, A. S., MacGregor, B. J., & Teske, A. (2016). Phylogeography, salinity adaptations and metabolic potential of the candidate division KB1 bacteria based on a partial single cell genome. *Frontiers in Microbiology*, *7*(1266), 1266. https://doi.org/10.3389/fmicb.2016.01266

Noah, M., Lappe, M., Schneider, B., Vieth-Hillebrand, A., Wilkes, H., & Kallmeyer, J. (2014). Tracing biogeochemical and microbial variability over a complete oil sand mining and recultivation process. *Science of the Total Environment*, *499*, 297–310. https://doi.org/10.1016/j.scitotenv.2014.08.020

Oren, A. (2002). Molecular ecology of extremely halophilic Archaea and Bacteria. *FEMS Microbiology Ecology*, *39*(1), 1–7. https://doi.org/10.1111/j.1574-6941.2002.tb00900.x

Oren, A. (2008). Microbial life at high salt concentrations: Phylogenetic and metabolic diversity. *Saline Systems*, *4*(1), 2. https://doi.org/10.1186/1746-1448-4-2

Oren, A. (2010). Microbial metabolism: Importance for environmental biotechnology. In L. K. Wang, V. Ivanov, & J.-H. Tay (Eds.), *Environmental Biotechnology* (pp. 193–255). Totowa, NJ: Humana Press. https://doi.org/10.1007/978-1-60327-140-0_5

Oren, A. (2014). Taxonomy of halophilic Archaea: Current status and future challenges. *Extremophiles*, *18*(5), 825–834. https://doi.org/10.1007/s00792-014-0654-9

Pease, T. K., Van Vleet, E. S., Barre, J. S., & Dickins, H. D. (1998). Simulated degradation of glyceryl ethers by hydrous and flash pyrolysis. *Organic Geochemistry*, *29*(4), 979–988. https://doi.org/10.1016/S0146-6380(98)00047-3

Pen-Mouratov, S., Hu, C., Hindin, E., & Steinberger, Y. (2011). Soil microbial activity and a free-living nematode community in the playa and in the sandy biological crust of the Negev Desert. *Biology and Fertility of Soils*, *47*(4), 363–375. https://doi.org/10.1007/s00374-011-0540-x

Piotrowska-Seget, Z., & Mrozik, A. (2003). Signature lipid biomarker (SLB) analysis in determining changes in community structure of soil microorganisms. *Polish Journal of Environmental Studies*, *12*(6), 669–675.

Pitcher, A., Hopmans, E. C., Schouten, S., & Damste, J. S. S. (2009). Separation of core and intact polar archaeal tetraether lipids using silica columns: Insights into living and fossil biomass contributions. *Organic Geochemistry*, *40*(1), 12–19. https://doi.org/10.1016/j.orggeochem.2008.09.008

Pointing, S. B., & Belnap, J. (2012). Microbial colonization and controls in dryland systems. *Nature Reviews Microbiology*, *10*(8), 551–562. https://doi.org/10.1038/nrmicro2831

Radke, M., Willsch, H., & Welte, D. H. (2002). Preparative hydrocarbon group type determination by automated medium pressure liquid chromatography. *Analytical Chemistry*, *52*(3), 406–411. https://doi.org/10.1021/ac50053a009

Ramette, A. (2007). Multivariate analyses in microbial ecology. *FEMS Microbiology Ecology*, *62*(2), 142–160. https://doi.org/10.1111/j.1574-6941.2007.00375.x

Ramisch, A., Bens, O., Buylaert, J. P., Eden, M., Heine, K., Hurkamp, K., et al. (2017). Fluvial landscape development in the southwestern Kalahari during the Holocene—Chronology and provenance of fluvial deposits in the Molopo Canyon. *Geomorphology*, *281*, 94–107. https://doi.org/10.1016/j.geomorph.2016.12.021

Rilfors, L., Wieslander, A., & Stahl, S. (1978). Lipid and protein composition of membranes of Bacillus megaterium variants in the temperature range 5 to 70 degrees C. *Journal of Bacteriology*, *135*(3), 1043–1052.

Roy, P. D., Smykatz-Kloss, W., & Sinha, R. (2006). Late Holocene geochemical history inferred from Sambhar and Didwana playa sediments, Thar Desert, India: Comparison and synthesis. *Quaternary International*, *144*(1), 84–98. https://doi.org/10.1016/j.quaint.2005.05.018

Russell, N. J. (1989). Adaptive modifications in membranes of halotolerant and halophilic microorganisms. *Journal of Bioenergetics and Biomembranes*, *21*(1), 93–113. https://doi.org/10.1007/BF00762214

Sankaranarayanan, K., Lowenstein, T. K., Timofeeff, M. N., Schubert, B. A., & Lum, J. K. (2014). Characterization of ancient DNA supports long-term survival of Haloarchaea. *Astrobiology*, *14*(7), 553–560. https://doi.org/10.1089/ast.2014.1173

Scanlon, B. R., Stonestrom, D. A., Reedy, R. C., Leaney, F. W., Gates, J., & Cresswell, R. G. (2009). Inventories and mobilization of unsaturated zone sulfate, fluoride, and chloride related to land use change in semiarid regions, southwestern United States and Australia. *Water Resources Research*, *45*, W00A18. https://doi.org/10.1029/2008WR006963

Schaechter, M. (2009). *Encyclopedia of microbiology*. San Diego, CA: Elsevier Science.

Schefuss, E., Kuhlmann, H., Mollenhauer, G., Prange, M., & Patzold, J. (2011). Forcing of wet phases in southeast Africa over the past 17,000 years. *Nature*, *480*(7378), 509–512. https://doi.org/10.1038/nature10685

Schirmack, J., Alawi, M., & Wagner, D. (2015). Influence of Martian regolith analogs on the activity and growth of methanogenic archaea, with special regard to long-term desiccation. *Frontiers in Microbiology*, *6*, 210. https://doi.org/10.3389/fmicb.2015.00210

Schouten, S., Hopmans, E. C., & Damste, J. S. S. (2013). The organic geochemistry of glycerol dialkyl glycerol tetraether lipids: A review. *Organic Geochemistry*, *54*, 19–61. https://doi.org/10.1016/j.orggeochem.2012.09.006

Schroeter, R., Hoffmann, T., Voigt, B., Meyer, H., Bleisteiner, M., Muntel, J., et al. (2013). Stress responses of the industrial workhorse Bacillus licheniformis to osmotic challenges. *PLoS One*, *8*(11), e80956. https://doi.org/10.1371/journal.pone.0080956

Schüller, I., & Wehrmann, A. (2016). Age determinations of Witpan sediment sequence (Northern Cape, South Africa) by 14C dating of TOC bulk samples: https://doi.org/10.1594/PANGAEA.865053

Schüller, I., & Wehrmann, A. (2017). Grain sizes of Omongwa Pan sediment sequence (Omaheke Region, Namibia) by Horiba Scattering Particle Size Distribution Analyzer LA-950. https://doi.org/10.1594/PANGAEA.882208

Shen, J. P., Zhang, L. M., Zhu, Y. G., Zhang, J. B., & He, J. Z. (2008). Abundance and composition of ammonia-oxidizing bacteria and ammonia-oxidizing archaea communities of an alkaline sandy loam. *Environmental Microbiology*, *10*(6), 1601–1611. https://doi.org/10.1111/j.1462-2920.2008.01578.x

Sime, L. C., Kohfeld, K. E., Le Quere, C., Wolff, E. W., de Boer, A. M., Graham, R. M., & Bopp, L. (2013). Southern Hemisphere westerly wind changes during the Last Glacial Maximum: Model-data comparison. *Quaternary Science Reviews*, *64*, 104–120. https://doi.org/10.1016/j.quascirev.2012.12.008

Smith, M., & Compton, J. S. (2004). Origin and evolution of major salts in the Darling pans, Western Cape, South Africa. *Applied Geochemistry*, *19*(5), 645–664. https://doi.org/10.1016/j.apgeochem.2003.10.003

Sogin, M. L., Morrison, H. G., Huber, J. A., Mark Welch, D., Huse, S. M., Neal, P. R., et al. (2006). Microbial diversity in the deep sea and the underexplored "rare biosphere". *Proceedings of the National Academy of Sciences of the United States of America*, *103*(32), 12,115–12,120. https://doi.org/10.1073/pnas.0605127103

Spain, A. M., Krumholz, L. R., & Elshahed, M. S. (2009). Abundance, composition, diversity and novelty of soil Proteobacteria. *The ISME Journal*, *3*(8), 992–1000. https://doi.org/10.1038/ismej.2009.43

Stomeo, F., Valverde, A., Pointing, S. B., McKay, C. P., Warren-Rhodes, K. A., Tuffin, M. I., et al. (2013). Hypolithic and soil microbial community assembly along an aridity gradient in the Namib Desert. *Extremophiles*, *17*(2), 329–337. https://doi.org/10.1007/s00792-013-0519-7

Telfer, M. W., Thomas, D. S. G., Parker, A. G., Walkington, H., & Finch, A. A. (2009). Optically Stimulated Luminescence (OSL) dating and palaeoenvironmental studies of pan (playa) sediment from Witpan, South Africa. *Palaeogeography Palaeoclimatology Palaeoecology*, *273*(1–2), 50–60. https://doi.org/10.1016/j.palaeo.2008.11.012

Thomas, F., Hehemann, J. H., Rebuffet, E., Czjzek, M., & Michel, G. (2011). Environmental and gut bacteroidetes: The food connection. *Frontiers in Microbiology*, *2*, 93. https://doi.org/10.3389/fmicb.2011.00093

Turich, C., & Freeman, K. H. (2011). Archaeal lipids record paleosalinity in hypersaline systems. *Organic Geochemistry*, *42*(9), 1147–1157. https://doi.org/10.1016/j.orggeochem.2011.06.002

Ventosa, A., Nieto, J. J., & Oren, A. (1998). Biology of moderately halophilic aerobic bacteria. *Microbiology and Molecular Biology Reviews*, *62*(2), 504–544.

Ventosa, A., Oren, A., & Ma, Y. (2011). *Halophiles and hypersaline environments: Current research and future trends*. Berlin: Springer.

Vieth, A., Mangelsdorf, K., Sykes, R., & Horsfield, B. (2008). Water extraction of coals—Potential for estimating low molecular weight organic acids as carbon feedstock for the deep terrestrial biosphere. *Organic Geochemistry*, *39*(8), 985–991. https://doi.org/10.1016/j.orggeochem.2008.02.012

Wang, H. Y., Liu, W. G., Zhang, C. L. L., Liu, Z. H., & He, Y. X. (2013). Branched and isoprenoid tetraether (BIT) index traces water content along two marsh-soil transects surrounding Lake Qinghai: Implications for paleo-humidity variation. *Organic Geochemistry*, *59*, 75–81. https://doi.org/10.1016/j.orggeochem.2013.03.011

Weijers, J. W. H., Schouten, S., Spaargaren, O. C., & Damste, J. S. S. (2006). Occurrence and distribution of tetraether membrane lipids in soils: Implications for the use of the TEX86 proxy and the BIT index. *Organic Geochemistry*, *37*(12), 1680–1693. https://doi.org/10.1016/j.orggeochem.2006.07.018

Weijers, J. W. H., Schouten, S., van den Donker, J. C., Hopmans, E. C., & Damste, J. S. S. (2007). Environmental controls on bacterial tetraether membrane lipid distribution in soils. *Geochimica et Cosmochimica Acta*, *71*(3), 703–713. https://doi.org/10.1016/j.gca.2006.10.003

White, D. C., Davis, W. M., Nickels, J. S., King, J. D., & Bobbie, R. J. (1979). Determination of the sedimentary microbial biomass by extractible lipid phosphate. *Oecologia*, *40*(1), 51–62. https://doi.org/10.1007/BF00388810

Zelles, L. (1999). Fatty acid patterns of phospholipids and lipopolysaccharides in the characterisation of microbial communities in soil: A review. *Biology and Fertility of Soils*, *29*(2), 111–129. https://doi.org/10.1007/s003740050533

Zhang, J., Kobert, K., Flouri, T., & Stamatakis, A. (2014). PEAR: A fast and accurate Illumina Paired-End reAd mergeR. *Bioinformatics*, *30*(5), 614–620. https://doi.org/10.1093/bioinformatics/btt593

Zhao, X. Q., Dupont, L., Schefuss, E., Meadows, M. E., Hahn, A., & Wefer, G. (2016). Holocene vegetation and climate variability in the winter and summer rainfall zones of South Africa. *Holocene*, *26*(6), 843–857. https://doi.org/10.1177/0959683615622544

Zink, K. G., & Mangelsdorf, K. (2004). Efficient and rapid method for extraction of intact phospholipids from sediments combined with molecular structure elucidation using LC-ESI-MS-MS analysis. *Analytical and Bioanalytical Chemistry*, *380*(5–6), 798–812. https://doi.org/10.1007/s00216-004-2828-2